ORIGINAL ARTICLE

β-Adrenergic blockade combined with subcutaneous B-type natriuretic peptide: a promising approach to reduce ventricular arrhythmia in heart failure?

Jérôme Thireau,[1] Sarah Karam,[1] Stéphanie Roberge,[1] Julien Roussel,[1] Franck Aimond,[1] Cécile Cassan,[1] Arnaud Gac,[2] Dominique Babuty,[3] Jean-Yves Le Guennec,[1] Alain Lacampagne,[1] Jérémy Fauconnier,[1] Sylvain Richard[1]

▶ Additional material is published online only. To view please visit the journal online (http://dx.doi.org/10.1136/heartjnl-2013-305167).

[1]Inserm U1046, Physiologie & Médecine Expérimentale, Cœur et Muscles, Université Montpellier-1 & 2, Montpellier, France
[2]ADInstruments Limited, Oxford, UK
[3]Service de Cardiologie, Hôpital Trousseau, Tours, France

Correspondence to
Dr Jérôme Thireau, Inserm U1046, Physiologie & Médecine Expérimentale, Cœur et Muscles, CHU Arnaud de Villeneuve, 371 avenue doyen G. Giraud, Montpellier 34295, France;
jerome.thireau@inserm.fr

SK and SR contributed equally to this study.

Received 28 October 2013
Revised 29 January 2014
Accepted 25 February 2014
Published Online First 25 March 2014

▶ http://dx.doi.org/10.1136/heartjnl-2014-305503

To cite: Thireau J, Karam S, Roberge S, *et al*. *Heart* 2014;**100**:833–841.

ABSTRACT

Aims Clinical studies failed to prove convincingly efficiency of intravenous infusion of neseritide during heart failure and evidence suggested a pro-adrenergic action of B-type natriuretic peptide (BNP). However, subcutaneous BNP therapy was recently proposed in heart failure, thus raising new perspectives over what was considered as a promising treatment. We tested the efficiency of a combination of oral β1-adrenergic receptor blocker metoprolol and subcutaneous BNP infusion in decompensated heart failure.

Methods and results The effects of metoprolol or/and BNP were studied on cardiac remodelling, excitation–contraction coupling and arrhythmias in an experimental mouse model of ischaemic heart failure following postmyocardial infarction. We determined the cellular and molecular mechanisms involved in anti-remodelling and antiarrhythmic actions. As major findings, the combination was more effective than metoprolol alone in reversing cardiac remodelling and preventing ventricular arrhythmia. The association of the two molecules improved cardiac function, reduced hypertrophy and fibrosis, and corrected the heart rate, sympatho-vagal balance (low frequencies/high frequencies) and ECG parameters (P to R wave interval (PR), QRS duration, QTc intervals). It also improved altered Ca^{2+} cycling by normalising Ca^{2+}-handling protein levels (S100A1, SERCA2a, RyR2), and prevented pro-arrhythmogenic Ca^{2+} waves derived from abnormal Ca^{2+} sparks in ventricular cardiomyocytes. Altogether these effects accounted for decreased occurrence of ventricular arrhythmias.

Conclusions Association of subcutaneous BNP and oral metoprolol appeared to be more effective than metoprolol alone. Breaking the deleterious loop linking BNP and sympathetic overdrive in heart failure could unmask the efficiency of BNP against deleterious damages in heart failure and bring a new potential approach against lethal arrhythmia during heart failure.

INTRODUCTION

A major source of preventable cardiac death in heart failure is the ventricular arrhythmia (VA).[1] VA involves ventricular remodelling and alterations of Ca^{2+} homeostasis following chronic adrenergic overactivation.[2] We showed that B-type natriuretic peptide (BNP) promotes Ca^{2+}-dependent VA via a similar mechanism.[3] The clinical advantages of the use of recombinant intravenous BNP nesiritide are also subject to debate despite its favourable haemodynamic effects.[4] One explanation could be that intravenous BNP further compromises autonomic regulation in heart failure[5 6] via a pro-adrenergic action unmasking its beneficial effects.[3 7 8]

Subcutaneous BNP administration has recently yielded promising results in systolic heart failure.[9] We thus aimed to determine the effects of a combination of the selective β1-adrenergic blocker (BB) metoprolol associated with subcutaneous BNP infusion in a mouse model of decompensated heart failure. Until now, no study in human or animal had specifically tested this combination and investigated cellular and molecular mechanisms. This combination could associate the efficiency of the main antiarrhythmic in use, particularly in postmyocardial ischaemic heart failure with a reduced LV EF,[10] and unmasks the beneficial antifibrotic, antiapoptotic and antihypertrophic properties of BNP by abolishing the BNP-associated adrenergic effects.

We showed that the combination was more effective than metoprolol or BNP alone in preventing cardiac remodelling and VA, with better benefits on cardiac morphology, function and Ca^{2+} homeostasis.

MATERIALS AND METHODS

Please refer online supplement for methods which is available online.

Study design

Procedures conformed to European Parliament Directive 2010/63/EU and Council on the protection of animals were approved by our institutional animal research committee (CE-LR-0714). Seven-week-old male C57Bl/6 mice (Janvier, France) were randomly assigned to the following groups: (1) postmyocardial infarction (PMI); (2) PMI treated with BNP (BNP-PMI); (3) PMI treated with metoprolol (BB-PMI); (4) PMI treated with metoprolol and BNP (BB-BNP-PMI); and (5) sham-operated mice (Shams). For PMI, the coronary artery was ligated 1–2 mm beyond its emergence from the left atrium, under anaesthesia and cardiac monitoring (2% isoflurane/O2, Aerrane, Baxter). Buprenorphine (0.3 mg/mL) was injected for postoperative analgesia.[3] Metoprolol (Sigma-Aldrich, 100 mg/kg/day) was administered in the drinking water. The mouse BNP (14-5-30A,

Heart: first published as 10.1136/heartjnl-2013-305167 on 25 March 2014. Downloaded from http://heart.bmj.com/ on April 20, 2024 by guest. Protected by copyright.

American Peptide, USA) was subcutaneously administered at 0.03 μg/kg/min for 14 days (Alzet-1002 osmotic pumps).[3] Following in vivo investigations, heart was explanted after cervical dislocation for single-cell experiments. The time sequence of the protocol is shown in figure 1.

In vivo analysis

Telemetric ECGs were recorded (DSI, USA) and analysed in respect of the Lambeth conventions. Heart rate variability, PR, QRS, corrected QT (QTc) intervals, short term variability of QT (QT_{STV}) and spontaneous arrhythmias were analysed (EMKA, France). To test the contribution of long term anti-remodelling effect of treatments on arrhythmogenic susceptibility, the β-adrenergic catecholamine isoproterenol (2.5 mg/kg intraperitoneal) was injected during and 4 weeks after the treatment. The triggering of sustained ventricular tachycardia (SVT) was monitored. At the same time-points, systolic, diastolic and mean arterial blood pressure were measured with a tail-cuff and pulse transducer (ML125/M NIBP System, ADInstruments, UK) in triplicate in conscious mice.

LV mass, LV shortening fraction, end-diastolic and end-systolic LV dimensions were measured by echocardiography (Vivid7Pro, GE Medical Systems, USA).[3] Survival throughout experimental protocol was followed (see online supplementary table S1 and S4).

Autopsy and heart excision

Autopsies were performed to verify pleural effusion and lungs congestion. The heart and lungs were excised and weighed, and the heart weight index determined (heart weight/body weight). Interstitial fibrosis was measured in 10 μm thick transverse sections of hearts in the peri-infarcted area (H&E and Sirius red staining). Results indicated the area of Sirius red-stained tissue (percentage of total area of myocardial tissue).

RNA extraction and RT-qPCR

Total RNA was extracted from LV tissue using TRIzol, and treated with DNase I at 37°C for 30 min. cDNA was synthesised using superscript II reverse transcriptase (Invitrogen, France). RT-qPCR was performed for myocardin-related transcription factor A (MRTF-A), serum response factor (SRF), Na^+-Ca^{2+} exchanger (NCX1), sarcoplasmic reticulum (SR) Ca^{2+}-ATPase (SERCA2a) and Ca^{2+}-binding protein S100a1 in duplicate (LightCycler, Roche, France) and normalised to GAPDH (eight mice/group).

Ca^{2+} handling and patch-clamp

Experiments were performed on freshly isolated LV myocytes.[3] Cardiomyocytes were loaded with Indo-1AM (10 μM, Invitrogen, France) and field-stimulated at 1.0 Hz with 1 ms current pulses (IonOptix system, USA).[3] Indo-1 fluorescence emitted at 405 (F405) and 480 nm (F480) were recorded to estimate intracellular Ca^{2+} level (F405 to F480 ratio) during a 30 s pacing period, followed by a 30 s rest period. Diastolic Ca^{2+} level, Ca^{2+} transient decay time (tau) and percentage of cells developing spontaneous Ca^{2+} waves were quantified during the rest period. Ca^{2+} sparks (frequency, amplitude and spatiotemporal characteristics) were recorded by following variations of fluorescence at 505 nm (ΔF) divided by initial fluorescence at 505 nm (F0) (ΔF/F0, Fluo-4AM, 5 μM, 1.5 ms/line; LSM510 Zeiss confocal microscope, 63X water-immersion objective, NA: 1.2). Cell volume was estimated using Z-stack (x-y projection, front view) image acquisition.[3] Electrophysiological profiles of cardiomyocytes were investigated by current-clamp (action potential (AP)) and voltage-clamp approaches ($I_{Ca,L}$, I_K) using the patch-clamp technique.

Ca^{2+}-handling proteins

LV were homogenised into lysis buffer (0.3% CHAPS, 1 μg/mL leupeptin, 1 μg/mL pepstatin and, in mM; HEPES 20, KCl 40, DTT 1, PMSF 1, EDTA 1, pH7.4) and centrifugated (6000×*g*, 5 min). After protein quantification (DC Protein Assay, Bio-Rad), total proteins (50 mg) were loaded on SDS-PAGE and transferred on nitrocellulose membrane (GE Healthcare). The membranes were blocked (Thermoscientific) and incubated with primary antibodies at 4°C overnight: SERCA2a (1:5000) (A010-20, Badrilla, UK), NCX1 (1:1000) (R3F1, Swant), ryanodine receptor RyR2 (1:1000) (Covalab, France) and PhosphoSer2808-RyR2 (1:1000) (A010-30, Badrilla), phospholamban (1:20 000) (A010-14, Badrilla) and PhosphoSer16-PLB (1:5000) (A010-12, Badrilla), and S100A1 (1:2500) (SP5355P, Acris antibodies, Germany). After incubation with secondary antibody 800 nm (1:30 000): antirabbit (SERCA2a, PhosphoPLB, RyR2, PhosphoRyR2, S100A1) or antimouse (NCX1, PLB, GAPDH), membranes were washed and scanned (Odyssey, LI-COR Biosciences). Results were expressed relative to GAPDH (1:60 000) (ab8245, Abcam).

STATISTICAL ANALYSIS

All data are reported as means±SD (mean±SE for patch-clamp experiments). Statistical analyses were performed using GraphPad Prism and Origin Softwares. One-way ANOVA for

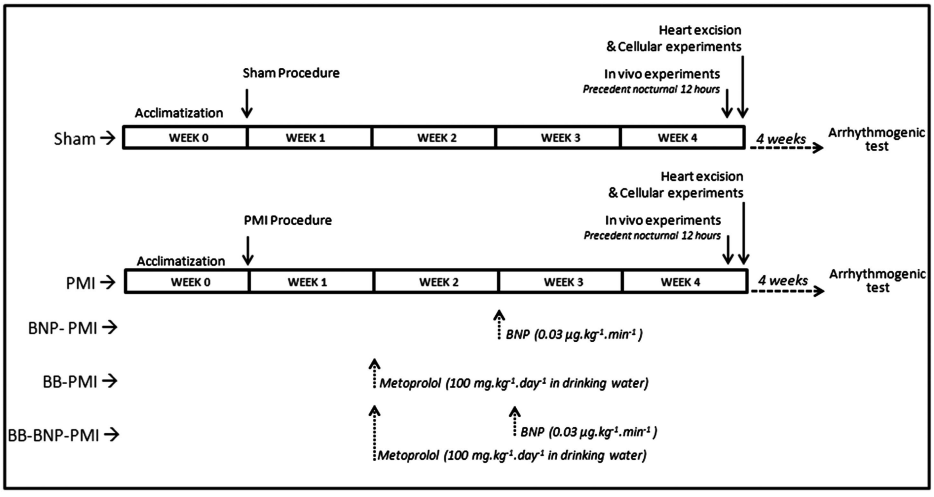

Figure 1 Time sequence of experimental procedure.

Heart: first published as 10.1136/heartjnl-2013-305167 on 25 March 2014. Downloaded from http://heart.bmj.com/ on April 20, 2024 by guest. Protected by copyright.

Table 1 Morphological and histological parameters

	Sham	PMI	BNP-PMI	BB-PMI	BB-BNP-PMI
Heart weight index (mg/g)	4.9±0.2	5.9±0.3‡	6.2±0.1‡	5.5±0.1†,§	5.3±1.1*,‖,¶
Pleural effusion (%)	0	58†	57†	69‡,§	33*,§,#
Lung congestion (%)	0	41†	42†	69‡,§	33*,§,#
LV end-diastolic dimension (mm)	25.4±0.5	52.4±0.4‡	47.1±0.3‡	42.1±0.5†,§	39.9±0.4†,§
LV shortening fraction (%)	58.9±1.3	17.4±1.1‡	17.5±0.8‡	24.6±0.6†,§	29.6±0.9†,‖,¶
Collagen (%)	0.1±0.0	5.2±1.8‡	3.6±0.2‡,§	4.6±1.9‡	2.4±1.5†,‖,¶
Cell volume (10^{-5} mm^3)	3.5±0.1	5.5±0.5‡	4.8±0.4†	4.3±0.3*,§	3.7±0.4‖,¶

Heart weight index. Percentage of animals exhibiting pleural effusion and lung congestion (15 mice/group). LV end-diastolic dimensions and shortening fraction (14 mice/group). Collagen content (percentage of the total area of myocardial tissue, 8 mice/group) and cell volume (n=30 cells, 3 mice/group). *,†,‡ p<0.05, p<0.01, p<0.001 versus Sham; §,‖ p<0.05, p<0.01 versus PMI; ¶,# p<0.05, p<0.01 versus BB-PMI.
BB, β1-adrenergic blocker; BNP, B-type natriuretic peptide; PMI, postmyocardial infarction.

Table 2 ECG analysis

	Sham	PMI	BNP-PMI	BB-PMI	BB-BNP-PMI
ECG parameters					
Heart rate (bpm)	593±11	630±12*	665±10†,§	536±12*,‖	539±12*,‖
QRS duration (ms)	17.4±1.1	32.8±1.4†	33.1±1.1†	33.5±1.2†	28.2±0.9*,§,¶
QTc interval (ms)	32.2±1.3	51.3±1.4†	59.5±1.6‡	46.4±3.2†,§	45.7±2.4†,§
QT_{STV} (ms)	178±34	362±31†	454±45†	285±33‡,§	149±55‖,¶
Heart rate variability					
LF (ms^2)	0.052±0.005	0.012±0.009†	0.009±0.004†	0.028±0.005†,§	0.041±0.004*,‖,¶
HF (ms^2)	0.032±0.005	0.028±0.009	0.025±0.006	0.032±0.005	0.033±0.009
LF to HF	1.62±0.11	0.43±0.12†	0.36±0.28†	0.87±0.27*,§	1.24±0.19*,‖,¶
SDNN (ms)	14.9±2.4	9.1±1.4*	5.8±1.3†	13.5±2.1§	18.1±2.1‖,¶
RMSSD (ms)	5.7±0.9	3.18±0.8*	3.54±1.1*	3.7±1.0*	3.6±1.1*
VA					
Number of VA	21.3±4.2	44.7±3.1†	56.2±2.7†	28.3±4.2§	16.6±2.4‖,¶
SVT (%)					
During treatment	8	50†	66‡,§	0‖	8‖
After treatment	0	58†	58†	33§	8‖,¶

BB+BNP improved heart rate variability and were more efficient than metoprolol alone to prevent variability of ventricular repolarisation and VA. Parameters estimated from 12 h nocturnal ECG: heart rate, QRS duration, corrected QT interval (QTc) and short term variability of QT (QT_{STV}). Heart rate variability analysis in the frequency- and time-domain with low frequencies (LF), high frequencies (HF) spectral power, LF to HF ratio, SD of all normal R-R intervals (SDNN) and square root of the mean square successive differences between successive normal R-R intervals (RMSSD). Number of spontaneous ventricular extrasystoles (VA) developed over 12 h ECG recording. Percentage of mice developing SVT following injection of isoproterenol (2.5 mg/kg intraperitoneal) during and assessed 4 weeks after treatment. *,†,‡ p<0.05, p<0.01, p<0.001 versus Sham; §,‖ p<0.05, p<0.01 versus PMI; ¶ p<0.05 versus BB-PMI; n=15/group.
BB, β1-adrenergic blocker; BNP, B-type natriuretic peptide; PMI, postmyocardial infarction; SVT, sustained ventricular tachycardia; VA, ventricular arrhythmia.

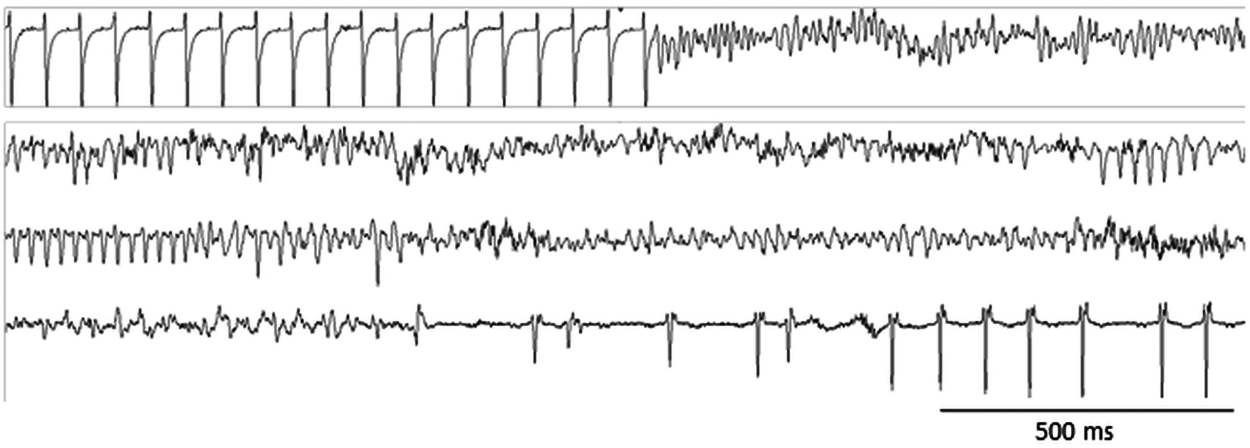

Figure 2 Arrhythmic events. Typical sustained ventricular tachycardia and ventricular fibrillation in postmyocardial infarction mice during isoproterenol challenge (2.5 mg/kg intraperitoneal).

Heart: first published as 10.1136/heartjnl-2013-305167 on 25 March 2014. Downloaded from http://heart.bmj.com/ on April 20, 2024 by guest. Protected by copyright.

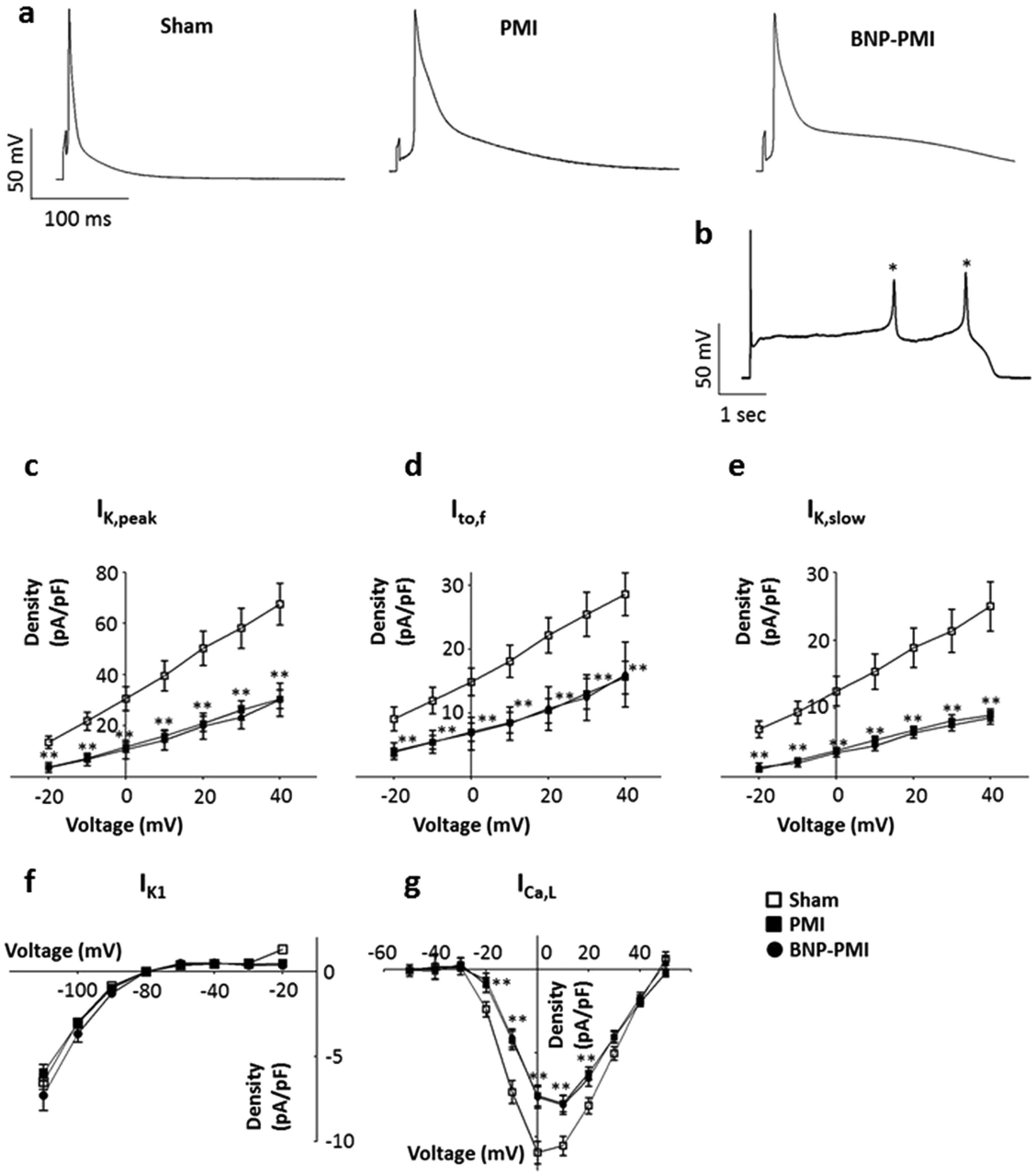

Figure 3 Cellular electrophysiological profiles. Current clamp studies: (A) Representative action potentials were recorded from LV cardiomyocytes isolated from Sham, postmyocardial infarction (PMI) and B-type natriuretic peptide (BNP)-PMI mice. (B) Typical early afterdepolarisations obtained in BNP-PMI mice. Voltage clamp studies: Ionic currents in Sham (open square), PMI (filled square) and BNP-PMI mice (filled circle). (C) Mean±SE current/voltage relationships of the total voltage-gated K^+ currents (I_{Kpeak}), (D) transient outward K^+ current ($I_{to,F}$), (E) I_{Kslow}, (F) I_{K1} and (G) $I_{Ca,L}$ (n=13–22 cells). **p<0.01 versus Sham.

multiple comparisons was used, followed by a parametric t test with Bonferroni's correction. Percentage data were analysed by a χ^2 test. A p value of 0.05 or less indicates a statistically significant difference.

RESULTS

BNP reduced fibrosis and metoprolol improved cardiac remodelling

MI mice exhibited heart failure with cardiac hypertrophy, increased LV end-diastolic dimensions, decreased LV shortening fraction and interstitial fibrosis (table 1; see online supplementary figure S1). The systolic, diastolic and mean arterial blood pressures were decreased (see online supplementary table S1). BNP did not improve morpho-functional remodelling after MI but reduced interstitial fibrosis (table 1, see online supplementary figure S1). In contrast, metoprolol reversed the increases of the heart weight index and LV end-diastolic dimensions in PMI, while pleural effusion and lung congestion worsened (table 1). Consistently, metoprolol reduced cell hypertrophy as confirmed by the quantification of MRTF-A and SRF mRNAs (see online supplementary table S2).

BB+BNP normalised morpho-functional parameters

The BB+BNP combination was far more effective than metoprolol on cardiac hypertrophy, pleural effusion, lung congestion and LV end-diastolic dimensions (table 1). The combination reduced fibrosis and hypertrophy more efficiently than BB (table 1, see online supplementary figure S1). BB and BB+BNP had no

Heart: first published as 10.1136/heartjnl-2013-305167 on 25 March 2014. Downloaded from http://heart.bmj.com/ on April 20, 2024 by guest. Protected by copyright.

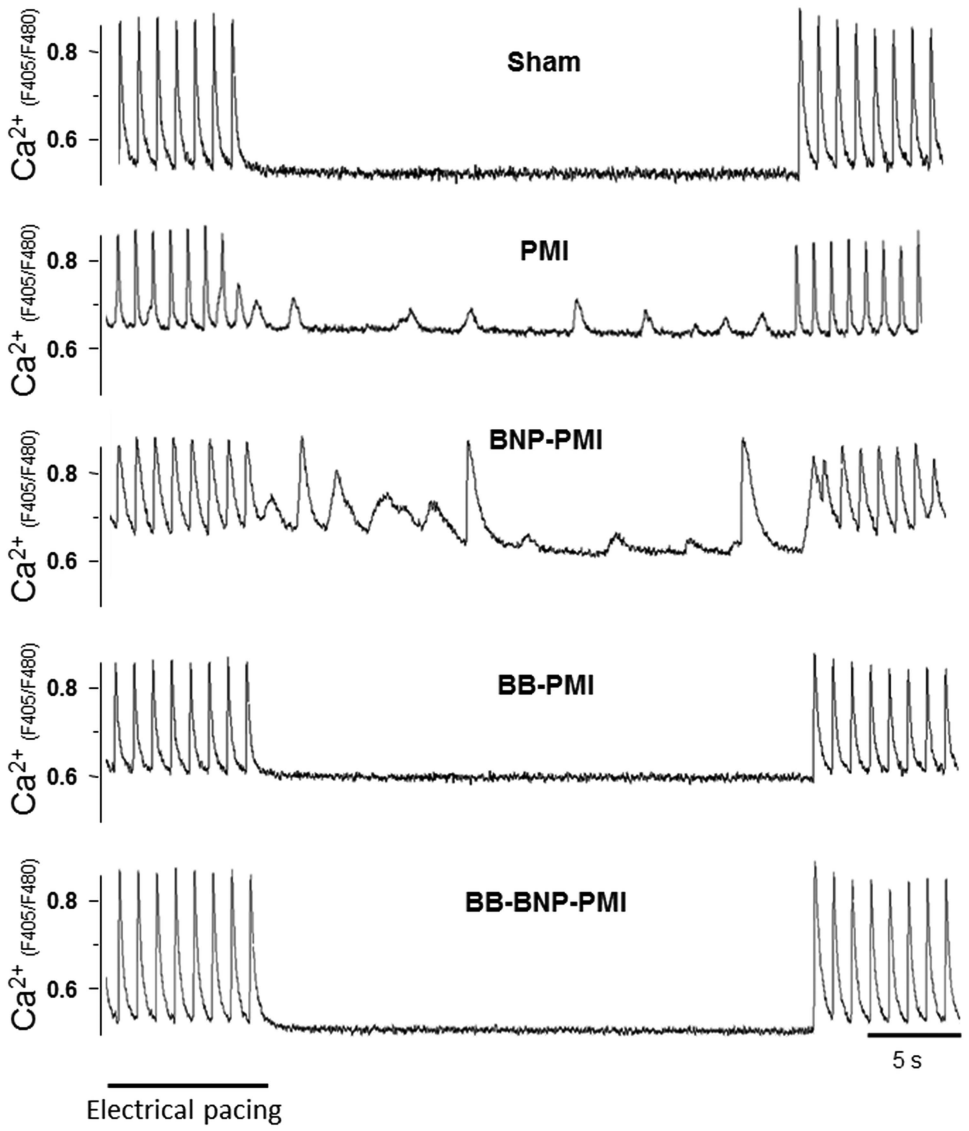

Figure 4 Ca^{2+} transients. BB+B-type natriuretic peptide (BNP) decreased cellular susceptibility to arrhythmia by normalising Ca^{2+} homeostasis. Indo1-AM fluorescence ratio at 405 and 480 nm (F405 to F480) reflected intracellular Ca^{2+} level variations during and after electrical pacing in LV cardiomyocytes. Postmyocardial infarction (PMI) and BNP-PMI developed abnormal spontaneous activities during non-stimulated period. BB, β1-adrenergic blocker.

detrimental effect on the systolic blood pressure during treatment and conferred a persistent beneficial effect over time (see online supplementary table S1).

BB+BNP corrected rhythm disturbances better than monotherapy

PMI mice presented higher heart rate, and prolonged QRS and QTc intervals (table 2) when compared with Shams. The typical collapsed low frequencies to high frequencies ratio indicated that the sympathetic system was overactivated, as observed in heart failure.[3] Moreover, the ventricular repolarisation instability expressed as the QT_{STV} was increased (table 2, see online supplementary figure S2). All these parameters are well-recognised prognostic markers for VA. PMI mice displayed a higher incidence of VA than Shams. BB and BB+BNP both normalised the heart rate and improved heart rate variability in PMI (table 2). The QT_{STV} and the number of VA were also diminished (table 2, see online supplementary figure S2). Similar results have been reported in heart failure patients under β-blockers.[11] Overall, BB+BNP was more effective than BB in correcting the heart rate variability and QT_{STV} and in reducing VA (table 2).

Since catecholamines are a potent trigger of VA, mice were challenged with isoproterenol at two time-points. (1) During treatment, 33% PMI and 66% BNP-PMI mice developed SVT whereas Sham did not (table 2). BB and BB+BNP prevented SVT. (2) When all treatments were stopped, 58% of PMI developed SVT, and 33% triggered ventricular fibrillation (figure 2, table 2). In the BNP-PMI group, 60% of mice developed SVT, and 33% developed ventricular fibrillation followed by cardiac death (4/12, $p<0.05$, χ^2 test vs PMI). The BB+BNP therapy remained highly beneficial in successfully preventing SVT (8%) (χ^2 test, $p<0.05$, table 2).

BB+BNP normalised intracellular Ca^{2+} homeostasis

VA could originate from AP lengthening and/or disturbed Ca^{2+} handling. Whereas AP shape was altered in PMI and BNP-PMI, AP duration and underlying currents (Ca^{2+} and K^+) were

Heart: first published as 10.1136/heartjnl-2013-305167 on 25 March 2014. Downloaded from http://heart.bmj.com/ on April 20, 2024 by guest. Protected by copyright.

Table 3 Intracellular Ca^{2+} signalling in LV cardiomyocytes, Ca^{2+} transients and cell shortening

	Sham	PMI	BNP-PMI	BB-PMI	BB-BNP-PMI
Ca^{2+} transient (Indo1-AM)					
Amplitude (F405 to F480)	5.24±0.18	4.47±0.25*	4.12±0.09†	5.3±0.11§	5.81±0.16*,‖,¶
τ (ms)	294±21	371±15*	361±17*	312±18§	262±19‖,#
SR-Ca^{2+} content (F405 to F480)	9.3±0.4	7.2±0.1*	6.4±0.3†,§	8.6±0.3§	9.6±0.2‖,#
Diastolic Ca^{2+} level (F405 to F480)	0.55±0.01	0.65±0.02†	0.71±0.01‡	0.51±0.02‖	0.50±0.01‖
Sarcomere shortening (%)	9.65±0.32	7.21±0.35†	7.06±0.34†	9.16±0.31§	10.41±0.29‖,#
Arrhythmic cells (%)	7.1±5.4	72.3±14.4‡	62.9±9.7‡	24.4±3.3*,¶	11.6±4.9¶,#
Ca^{2+} sparks (Fluo4-AM)					
Frequency (Events.100/μm/S)	1.05±0.05	5.12±0.23†	6.34±0.13†,§	1.84±0.14*,‖	1.04±0.27¶,#
Amplitude (ΔF/F0)	0.58±0.01	0.49±0.02*	0.41±0.01†,‖	0.54±0.01§	0.61±0.01¶,#
FDHM (ms)	14.3±0.4	23.7±1.2†	34.3±2.1†,‖	16.9±1.7*,§	11.1±1.1¶,#
FWHM (ms)	1.34±0.02	1.67±0.05*	2.10±0.06†	1.50±0.05	1.59±0.04

BB+BNP decreased cellular susceptibility to arrhythmia by normalising Ca^{2+} homeostasis. Averaged Ca^{2+} transient amplitudes expressed as Indo1-AM fluorescence (F405/F480), averaged decay time constants (τ) of Ca^{2+} transients, averaged sarcoplasmic reticulum (SR)-Ca^{2+}content following caffeine application, averaged diastolic Ca^{2+} levels, sarcomeres shortening (%) and percentage of cells exhibiting spontaneous irregular Ca^{2+} waves (n=50 cells, 5 mice/group). Ca^{2+} sparks. BB+BNP prevented Ca^{2+} leakage from RyR2. Averaged Ca^{2+} spark frequencies detected by Fluo4-AM fluorescence. Ca^{2+} sparks amplitude (variation of fluorescence at 505 nm/initial fluorescence at 505 nm, ΔF/F0), full width (FWHM) and full duration (FDHM) at half maximum of Ca^{2+} sparks (n=60 cells, 6 mice/group). *,†,‡ p<0.05, p<0.01, p<0.001 versus Sham; §,‖,¶ p<0.05, p<0.01, p<0.001 versus PMI animals; # p<0.05 versus BB-PMI animals.
BB, β1-adrenergic blocker; BNP, B-type natriuretic peptide; PMI, postmyocardial infarction.

comparable between these two groups (figure 3, see online supplementary table S3). So we looked for differences in intracellular Ca^{2+} level that could trigger afterdepolarisations (figure 3B). In PMI, Ca^{2+} transient was altered with smaller amplitude and slower decay kinetics together with reduced SR-Ca^{2+} content and higher diastolic Ca^{2+} levels than in Shams (figure 4, table 3). These changes accounted for, respectively, the decrease in sarcomeres shortening and the triggering of spontaneous irregular Ca^{2+} waves (figure 4, table 3). Chronic BNP worsened all these alterations and irregular Ca^{2+} waves persisted (figure 4, table 3). In contrast, both BB and BB+BNP improved Ca^{2+} homeostasis and reduced the number of pro-arrhythmogenic waves (table 3). Nevertheless, BB+BNP was more effective than BB alone to reduce Ca^{2+} sparks frequency and occurrence of Ca^{2+} waves (figure 4 and figure 5; table 3). Thus, the beneficial effects of BB+BNP on Ca^{2+} cycling could explain its antiarrhythmic advantage.

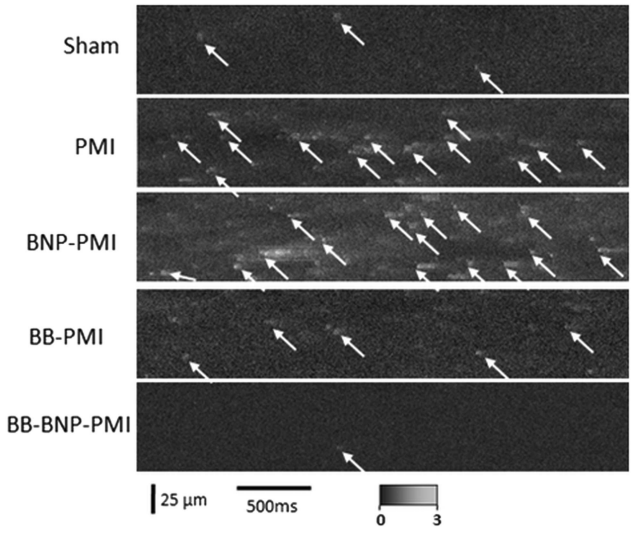

Figure 5 Ca^{2+} sparks. BB+B-type natriuretic peptide (BNP) prevented Ca^{2+} leakage from RyR2. Representative variations of fluorescence at 505 nm (F505) during line scan acquisition in Fluo-4 AM-loaded cardiomyocytes from Sham, postmyocardial infarction (PMI), BNP-PMI, BB-PMI and BB-BNP-PMI animals. Each sporadic elevation of fluorescence (indicated by white arrows) represents a Ca^{2+} spark due to spontaneous activation of ryanodine receptors. Whereas Sham cells presented few Ca^{2+} sparks, PMI presented an increased sparks frequency, reflecting a severe Ca^{2+} leakage from the reticulum sarcoplasmic. BB and, to a larger extent, BB-BNP reduced Ca^{2+} sparks frequency. BB, β1-adrenergic blocker.

BB+BNP normalised changes in Ca^{2+}-handling proteins

The alterations of Ca^{2+} homeostasis in heart failure resulted from modifications of Ca^{2+}-handling proteins as we observed for SERCA2a, S100A1 and NCX in PMI (table 4, see online supplementary figure S3). In addition, PLB phosphorylation (Ser16) was decreased while RyR2 phosphorylation (Ser2808) was increased (table 4). BNP had no major effect on SERCA2a, NCX, or the phosphorylation of PLB and RyR2, but it further reduced S100A1 expression (table 4, see online supplementary figure S3). This additional reduction of S100A1 accounted for the higher Ca^{2+} sparks frequency in BNP-PMI.[12 13] In contrast, BB+BNP normalised SERCA2a, NCX and S100A1 expression, and the phosphorylation of PLB and RyR2 (table 4, see online supplementary figure S3). The benefits of BB were therefore enhanced by BNP, with an additional decrease in NCX1 expression and the P-RyR2 to RyR2 ratio, and normalisation of PLB phosphorylation. These results accounted for the improved control of Ca^{2+} leakage and inotropy, and prevention of irregular Ca^{2+} waves.

DISCUSSION

β-Blockers are commonly used as first-line treatment after MI and heart failure, with unquestionable benefits on mortality.[14] Here, we conclude that a combination of the selective BB metoprolol with subcutaneous BNP is more effective to prevent cardiac remodelling than metoprolol alone in decompensated heart failure. We also provide novel insights into how the combination prevents Ca^{2+}-handling alterations and subsequent morbid arrhythmias (figure 6).

Heart: first published as 10.1136/heartjnl-2013-305167 on 25 March 2014. Downloaded from http://heart.bmj.com/ on April 20, 2024 by guest. Protected by copyright.

Table 4 Ca^{2+}-handling proteins

	Sham	PMI	BNP-PMI	BB-PMI	BB-BNP-PMI
SERCA2a (/GAPDH)	0.51±0.12	0.25±0.05*	0.24±0.09*	0.70±0.05*,‖	0.84±0.04†,‖
NCX1 (/GAPDH)	0.38±0.02	0.67±0.02†	0.61±0.02†	0.52±0.02*,§	0.43±0.04‖,¶
S100A1 (/GAPDH)	0.85±0.07	0.59±0.06†	0.49±0.03‡	0.72±.041‖	0.69±0.03‖
PSer16-PLB (/GAPDH)	1.00±0.03	0.54±0.01*	0.70±0.01*	1.53±0.02†,§,#	0.83±0.02
PLB (/GAPDH)	2.01±0.03	2.51±0.02*	2.42±0.02*	2.12±0.04§	1.64±0.02*,‖,#
PSer16-PLB to PLB ratio	0.49±0.01	0.17±0.02†	0.20±0.01†	0.72±0.01†,§	0.53±0.03‖,#
Pser2808-RyR (/GAPDH)	0.53±0.04	0.47±0.06	0.57±0.09	0.48±0.05	0.24±0.04
RyR (/GAPDH)	0.48±0.04	0.35±0.05*	0.61±0.09§	0.62±0.05*,§	0.48±0.03*,§,#
Pser2808-RyR to RyR ratio	1.12±0.09	1.51±0.10*	1.20±0.08	0.73±0.03*,‖	0.43±0.07†,¶,#

BB+BNP normalised expression and post-traductional modifications of Ca^{2+}-handling proteins. Normalised protein content to GAPDH for SERCA2a, NCX1, S100A1, PSer16-PLB, PLB, PSer2808-RyR and RyR. The ratio of PSer16-PLB to PLB and PSer2808-RyR to RyR were calculated. *,†,‡ p<0.05, p<0.01, p<0.001 versus Sham; §,‖,¶ p<0.05, p<0.01, p<0.001 versus PMI animals; # p<0.05 versus BB-PMI animals (n=10/group).
BB, β1-adrenergic blocker; BNP, B-type natriuretic peptide; PMI, postmyocardial infarction.

Higher benefits of BB+BNP on cardiac remodelling

Favourable effects of BNP have been reported in hypertension-induced heart failure,[15] but they are still debated in postischaemic heart failure.[16–18] We showed that subcutaneous BNP was beneficial when combined with metoprolol in ischaemic heart failure. Furthermore, the overall benefit was independent of heart rate and haemodynamic changes. In particular, no severe hypotension was observed.[4] The combination clearly associated the antifibrotic effect of BNP and the anti-remodelling action of metoprolol that account for efficient anti-arrhythmic properties. Even if in the ASCEND-HF trial almost 60% of patients received β-blocker therapy and/or ACE inhibitors with intravenous BNP infusion,[4] it is the first time that a study specifically addressed the utility to use subcutaneous BNP associated with oral metoprolol in heart failure and reveals beneficial effects. In the ASCEND-HF trial no benefit was observed. The discrepancy may reflect differences of dosage, administration route (intravenous 0.01 µg/kg/min for 24 h or more for up to 7 days in acute decompensated heart failure vs subcutaneous 0.03 µg/kg/min for 15 days in established chronic heart failure) and of model.

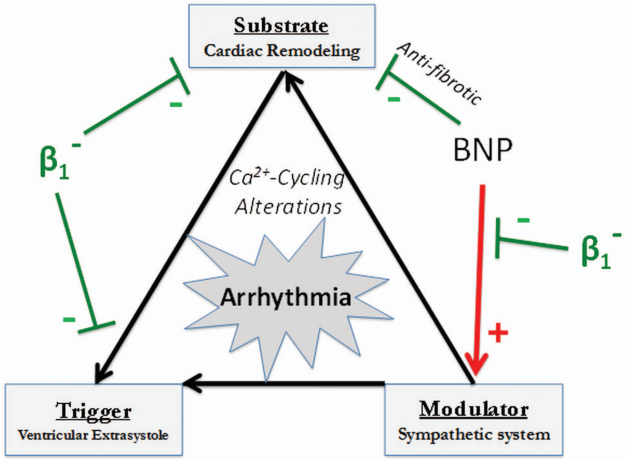

Figure 6 Beneficial effect of combination therapy in the concept of *Coumel*'s triangle of arrhythmogenesis.[30] In addition to its beneficial effects on the 'substrate' (cardiac remodelling) and the 'trigger' (Ca^{2+} cycling), β1-adrenergic receptor antagonism also abolishes the adverse consequences of B-type natriuretic peptide (BNP) on the 'modulator' (sympathetic system overactivation).

The normalisation of the sympatho-vagal balance by the combination was a key mechanism contributing to its overall therapeutic effect. Metoprolol not only provided its well-known benefits, but it broke the deleterious loop linking BNP and sympathetic overdrive.[3] Indeed, BNP promotes adrenergic signalling through two distinct pathways. BNP induces norepinephrine release from sympathetic cardiac neurons via protein kinase G-induced inhibition of PDE3-mediated cAMP hydrolysis,[7] which is likely to offset its desirable effects.[7 8 19] BNP also inhibits PDE3 through the activation of NPR-B,[8 20] which is the predominant natriuretic peptide receptor in failing hearts.[21] Moreover, whereas low doses of nesiritide have beneficial effect on autonomic nervous system, high doses of intravenous BNP could induce prolonged hypotension and activate the sympathetic system.[5 22] Altogether, these effects could account for the increased propensity of BNP-PMI mice to develop catecholamines-induced VT, fibrillation and death. Such pro-arrhythmic effect was observed in patients in whom high doses of intravenous nesiritide induced a minor increase of VA (ventricular tachcardia (VT), couplets and triplets).[23] However, in this study, the antiarrhythmic treatment of patients may have prevented the effect of parenteral vasoactive therapy on the occurrence of VAs.[23] In addition, non-sustained VT was also reported during study drug infusion of nesiritide in three patients receiving a high dose of nesiritide (0.03 µg/kg/min) in clinical trial.[22] We therefore propose that the combination retains the beneficial effects of subcutaneous BNP but attenuates the deleterious consequences mediated by β1-adrenergic pathway. In line, the combination reduced fibrosis and corrected the QRS lengthening and QT dispersion, which both correlate with a lowered risk of developing VA.[11 24] Importantly, this antiarrhythmic benefit persisted over time, and lasted longer than that of metoprolol alone, which is in line with a protective long-term anti-remodelling effect.

Mechanisms of higher benefits of BB+BNP combination therapy

Alterations in Ca^{2+} homeostasis are responsible for excitation–contraction coupling defects and VA.[2] Aberrant ryanodine receptor (RyR) opening in diastole, observed functionally as the abnormal occurrence of Ca^{2+} sparks, generates spontaneous irregular Ca^{2+} waves involved in the triggering of VA/SVT.[25 26] Increase in Ca^{2+} sparks frequency could result from increased cytosolic Ca^{2+} level due to a blunted SERCA2a activity, associated with a modulation of the intrinsic properties of the RyR2 complex (see online

Heart: first published as 10.1136/heartjnl-2013-305167 on 25 March 2014. Downloaded from http://heart.bmj.com/ on April 20, 2024 by guest. Protected by copyright.

supplement). Sympathetic overdrive, leading to SR-Ca^{2+} leakage, may be involved since high diastolic Ca^{2+} levels could also participate in the triggering of afterdepolarisations. The combination effectively reduced SR-Ca^{2+} leakage, and improved SR-Ca^{2+} load and transient amplitude by normalising proteins alterations which accounted for the maintained cell contraction and the antiarrhythmic properties. Interestingly, the combination restored baseline levels of S100A1 and increased SR-Ca^{2+} content. Restoration of S100A1 expression, as a Ca^{2+}-dependent molecular inotrope regulating cardiac SR-Ca^{2+} cycling, was suggested to treat heart failure.[27]

Clinical implication

The most important finding of this study is that association of oral metoprolol with subcutaneous BNP infusion is more effective than monotherapy with the β-blocker in reducing ventricular remodelling and VA following MI. The interest of combinations, elevating circulating plasma concentration of natriuretic peptides associated with classical drugs, has been recently highlighted.[28 29] For example, neutral endopeptidase inhibitors have per se limited clinical benefice. However, their association with ACE or angiotensin receptor antagonists is promising despite limitations such as incidence of multilevel potentially life-threatening angioedema.[28] Our results may challenge this innovative concept because β1-adrenergic receptor antagonisation abolished the main adverse effects of BNP (figure 6). The therapeutic benefits resulted from an improved balance of the BNP and adrenergic systems, and from mechanisms intrinsic to the two pathways at the cardiomyocytes level. These promising results obtained in an experimental model of ischaemic heart failure warrant further evaluation and optimisation (dose) in humans.

Key messages

What is already known on this subject

Chronic B-type natriuretic peptide (BNP) administration alters excitation–contraction coupling (Ca^{2+} signalling) in mouse ventricular cardiomyocytes, which triggers ventricular arrhythmia through activation of the sympathetic system. However, chronic subcutaneous BNP improves cardiac function and avoids the severe hypotensive effect of BNP.

What this study adds

We determined the effects of a combination of the selective β1-adrenergic blocker metoprolol associated with subcutaneous BNP infusion in a mouse model of decompensated heart failure. Until now, no study in humans or animals had specifically tested this combination and investigated both cellular and molecular mechanisms. We showed that metoprolol unmasks beneficial effects of BNP. The combination of the two molecules reduced the occurrence of both spontaneous and catecholamines-induced ventricular tachycardia in postischaemic heart failure.

Contributors (1) Conception and design or analysis and interpretation of data, or both, in addition to experimental work: JT, SK, SR, JR, CC, AG, JF, FA. (2) Drafting of the manuscript or revising it critically for important intellectual content: JT DB, J-Y LG, AL, SR. (3) Final approval of the manuscript submitted: JT, SR.

Funding This work was supported by *Fondation de France* (Project PepNaRhythm, N° 2068001722) and INSERM. JT, SR, JF and AL hold CNRS positions.

Competing interests None.

Provenance and peer review Not commissioned; externally peer reviewed.

REFERENCES

1 Roger VL, Go AS, Lloyd-Jones DM, *et al*. Heart disease and stroke statistics—2012 update: a report from the American Heart Association. *Circulation* 2012;125:e2–220.
2 Ikeda Y, Hoshijima M, Chien KR. Toward biologically targeted therapy of calcium cycling defects in heart failure. *Physiology (Bethesda)* 2008;23:6–16.
3 Thireau J, Karam S, Fauconnier J, *et al*. Functional evidence for an active role of B-type natriuretic peptide in cardiac remodelling and pro-arrhythmogenicity. *Cardiovasc Res* 2012;95:59–68.
4 O'Connor CM, Starling RC, Hernandez AF, *et al*. Effect of nesiritide in patients with acute decompensated heart failure. *N Engl J Med* 2011;365:32–43.
5 Aronson D, Burger AJ. Effect of nesiritide (human b-type natriuretic peptide) and dobutamine on heart rate variability in decompensated heart failure. *Am Heart J* 2004;148:e16.
6 Azevedo ER, Newton GE, Parker AB, *et al*. Sympathetic responses to atrial natriuretic peptide in patients with congestive heart failure. *J Cardiovasc Pharmacol* 2000;35:129–35.
7 Chan NY, Seyedi N, Takano K, *et al*. An unsuspected property of natriuretic peptides: promotion of calcium-dependent catecholamine release via protein kinase G-mediated phosphodiesterase type 3 inhibition. *Circulation* 2012;125:298–307.
8 Qvigstad E, Moltzau LR, Aronsen JM, *et al*. Natriuretic peptides increase beta1-adrenoceptor signalling in failing hearts through phosphodiesterase 3 inhibition. *Cardiovasc Res* 2010;85:763–72.
9 Chen HH, Glockner JF, Schirger JA, *et al*. Novel protein therapeutics for systolic heart failure: chronic subcutaneous B-type natriuretic peptide. *J Am Coll Cardiol* 2012;60:2305–12.
10 Hunt SA, Abraham WT, Chin MH, *et al*. ACC/AHA 2005 Guideline Update for the Diagnosis and Management of Chronic Heart Failure in the Adult: a report of the American College of Cardiology/American Heart Association Task Force on Practice Guidelines (Writing Committee to Update the 2001 Guidelines for the Evaluation and Management of Heart Failure): developed in collaboration with the American College of Chest Physicians and the International Society for Heart and Lung Transplantation: endorsed by the Heart Rhythm Society. *Circulation* 2005;112:e154–235.
11 Bonnar CE, Davie AP, Caruana L, *et al*. QT dispersion in patients with chronic heart failure: beta blockers are associated with a reduction in QT dispersion. *Heart* 1999;81:297–302.
12 Volkers M, Loughrey CM, Macquaide N, *et al*. S100A1 decreases calcium spark frequency and alters their spatial characteristics in permeabilized adult ventricular cardiomyocytes. *Cell Calcium* 2007;41:135–43.
13 Most P, Remppis A, Pleger ST, *et al*. S100A1: a novel inotropic regulator of cardiac performance. Transition from molecular physiology to pathophysiological relevance. *Am J Physiol Regul Integr Comp Physiol* 2007;293:R568–77.
14 Antman EM, Hand M, Armstrong PW, *et al*. 2007 Focused Update of the ACC/AHA 2004 Guidelines for the Management of Patients With ST-Elevation Myocardial Infarction: a report of the American College of Cardiology/American Heart Association Task Force on Practice Guidelines: developed in collaboration With the Canadian Cardiovascular Society endorsed by the American Academy of Family Physicians: 2007 Writing Group to Review New Evidence and Update the ACC/AHA 2004 Guidelines for the Management of Patients With ST-Elevation Myocardial Infarction, Writing on Behalf of the 2004 Writing Committee. *Circulation* 2008;117:296–329.
15 Cataliotti A, Tonne JM, Bellavia D, *et al*. Long-term cardiac pro-B-type natriuretic peptide gene delivery prevents the development of hypertensive heart disease in spontaneously hypertensive rats. *Circulation* 2011;123:1297–305.
16 Pan Y, Zhu W, Ma J, *et al*. Therapeutic effects of continuous infusion of brain natriuretic peptides on postmyocardial infarction ventricular remodelling in rats. *Arch Cardiovasc Dis* 2011;104:17–28.
17 He J, Chen Y, Huang Y, *et al*. Effect of long-term B-type natriuretic peptide treatment on left ventricular remodeling and function after myocardial infarction in rats. *Eur J Pharmacol* 2009;602:132–7.
18 George I, Xydas S, Klotz S, *et al*. Long-term effects of B-type natriuretic peptide infusion after acute myocardial infarction in a rat model. *J Cardiovasc Pharmacol* 2010;55:14–20.
19 Chan NY, Robador PA, Levi R. Natriuretic peptide-induced catecholamine release from cardiac sympathetic neurons: inhibition by histamine H3 and H4 receptor activation. *J Pharmacol Exp Ther* 2012;343:568–77.
20 Springer J, Azer J, Hua R, *et al*. The natriuretic peptides BNP and CNP increase heart rate and electrical conduction by stimulating ionic currents in the sinoatrial node and atrial myocardium following activation of guanylyl cyclase-linked natriuretic peptide receptors. *J Mol Cell Cardiol* 2012;52:1122–34.
21 Dickey DM, Flora DR, Bryan PM, *et al*. Differential regulation of membrane guanylyl cyclases in congestive heart failure: natriuretic peptide receptor (NPR)-B, Not NPR-A, is the predominant natriuretic peptide receptor in the failing heart. *Endocrinology* 2007;148:3518–22.
22 Mills RM, LeJemtel TH, Horton DP, *et al*. Sustained hemodynamic effects of an infusion of nesiritide (human b-type natriuretic peptide) in heart failure: a

Heart: first published as 10.1136/heartjnl-2013-305167 on 25 March 2014. Downloaded from http://heart.bmj.com/ on April 20, 2024 by guest. Protected by copyright.

randomized, double-blind, placebo-controlled clinical trial. Natrecor Study Group. *J Am Coll Cardiol* 1999;34:155–62.
23 Burger AJ, Horton DP, LeJemtel T, *et al*. Effect of nesiritide (B-type natriuretic peptide) and dobutamine on ventricular arrhythmias in the treatment of patients with acutely decompensated congestive heart failure: the PRECEDENT study. *Am Heart J* 2002;144:1102–8.
24 Hinterseer M, Beckmann BM, Thomsen MB, *et al*. Usefulness of short-term variability of QT intervals as a predictor for electrical remodeling and proarrhythmia in patients with nonischemic heart failure. *Am J Cardiol* 2010;106:216–20.
25 Cheng H, Lederer WJ. Calcium sparks. *Physiol Rev* 2008;88:1491–545.
26 Fauconnier J, Thireau J, Reiken S, *et al*. Leaky RyR2 trigger ventricular arrhythmias in Duchenne muscular dystrophy. *Proc Natl Acad Sci U S A* 2010;107:1559–64.
27 Brinks H, Rohde D, Voelkers M, *et al*. S100A1 genetically targeted therapy reverses dysfunction of human failing cardiomyocytes. *J Am Coll Cardiol* 2011;58:966–73.
28 Mangiafico S, Costello-Boerrigter LC, Andersen IA, *et al*. Neutral endopeptidase inhibition and the natriuretic peptide system: an evolving strategy in cardiovascular therapeutics. *Eur Heart J* 2013;34:886–93c.
29 von Lueder TG, Sangaralingham SJ, Wang BH, *et al*. Renin-Angiotensin blockade combined with natriuretic Peptide system augmentation: novel therapeutic concepts to combat heart failure. *Circ Heart Fail* 2013;6:594–605.
30 Coumel P. Cardiac arrhythmias and the autonomic nervous system. *J Cardiovasc Electrophysiol* 1993;4:338–55.

Heart: first published as 10.1136/heartjnl-2013-305167 on 25 March 2014. Downloaded from http://heart.bmj.com/ on April 20, 2024 by guest. Protected by copyright.

SUPPLEMENTAL MATERIAL

Beta-adrenergic blockade combined with subcutaneous B-type natriuretic peptide: A promising approach to reduce ventricular arrhythmia in heart failure?

Jérôme Thireau[*]||, Sarah Karam[*]†, Stéphanie Roberge[*]†, Julien Roussel[*], Franck Aimond[*], Cécile Cassan[*], Arnaud Gac‡, Dominique Babuty§, Jean-Yves Le Guennec[*], Alain Lacampagne[*], Jérémy Fauconnier[*], Sylvain Richard[*]

[*]Inserm U1046, *Physiologie & Médecine Expérimentale, Cœur et Muscles*, Université Montpellier-1 & Université Montpellier-2, Montpellier, France.
‡ADInstruments Limited, Oxford OX4 6HD, UK
§Hôpital Trousseau, Tours, France.

†*Equal contribution.*

|| **Corresponding author:** Dr. Jérôme Thireau

Inserm U1046, Physiologie & Médecine Expérimentale, Cœur et Muscles
CHU Arnaud de Villeneuve, 371 Rue du doyen G. Giraud, 34295 Montpellier

Phone: (33)04.67.41.52.22
Fax: (33)04.67.41.52.42
E-mail: jerome.thireau@inserm.fr

Methods

Animals and BNP

Seven-week-old male C57Bl/6 mice (Janvier, France) were randomly assigned to the following groups: 1) mice in post-myocardial infarction after left coronary artery ligation as previously described (PMI mice); 2) PMI mice treated with BNP (BNP-PMI); 3) PMI mice treated with metoprolol (BB-PMI); 4) PMI mice treated with metoprolol and BNP (BB-BNP-PMI) and 5) sham-operated mice (Shams).[1] For PMI, a left thoracotomy was performed under anesthesia and cardiac monitoring (2% isoflurane/O_2, Aerrane®, Baxter, France). The artery was ligated 1-2 mm beyond the emergence from the top of the left atrium, using an 8-0 suture. A subcutaneous injection of 0.01 ml buprenorphine solution (0.3 $mg.ml^{-1}$) for post-operative analgesia was administered. Shams were subjected to the same surgical procedure but without coronary artery ligation. Echocardiography was systematically realized before the inclusion of animal to ensure that ligation was correctly performed. Only animals surviving at day-5 post surgery and with comparable echocardiography parameters at this time were included in the study to limit bias due to differences in size infract. No animal died or had been sacrificed after inclusion in the study, and before the end of experiments due to achievement of endpoints (according to our ethics committee). Metoprolol (Sigma-Aldrich, $100mg.kg^{-1}.day.^{-1}$) was administered in the drinking water.[2] The active form of mouse BNP (Ref 14-5-30A, American Peptide, Sunnyvale, USA) was administered using a micro-osmotic pump (Alzet 1002, France, 0.03 $\mu g.kg^{-1}.min^{-1}$ for 14 days).[2] Circulating BNP levels were assessed on Day-28 (Phoenix Pharmaceuticals, Belmont, USA). BNP levels in Shams were inferior to 0.34 ng/ml. BNP levels increased to 5.1±0.9 ng/ml in PMI, 4.7±0.8 ng/ml in BB-PMI, 11.2±0.7 ng/ml in BNP-PMI, and 11.9±1.0 ng/ml in BB-BNP-PMI mice (n=8 per group). Following *in vivo* investigations, the heart was explanted after cervical dislocation for single-cell experiments. The time sequence of the protocol is available in the on-line supplement (**Figure 1**). All procedures conformed to European Parliament Directive 2010/63/EU and the 22 September 2010 Council on the protection of animals, and were approved by the institutional animal research committee (Departmental Directorate of protecting populations and animal health (ethics for animal welfare and environmental protection, N° A 34- 485) and by our Ethics committee for animal experiments, Languedoc Roussillon, N° CE-LR-0714).

Choice of the BNP dose.

In clinics, recommendations include an optional intravenous bolus of nesiritide for rapid haemodynamic changes in urgency at a dose of 2 $\mu g.kg^{-1}$ (administered at the discretion of the investigator) and a continuous infusion of 0.01 to 0.03 $\mu g.kg^{-1}.min^{-1}$ for 24 hours or more for up to 7 days. Dosage is also adjusted during chronic infusion to limit severe hypotension. In our study, animals were treated with continuous infusion of BNP for 14 days by means of micro-osmotic pumps (0.03 $\mu g.kg^{-1}.min^{-1}$). To our knowledge, no dose-effect relationship in mice was published on cardiac function from cellular to *in vivo* experiments in chronic conditions. In addition, no time-course of BNP release into circulation after coronary artery ligation was available. Thus we chose the dose and duration of exposure based on BNP dosages and on its associated effects published in our previous paper.[1] At this dose, BNP presented hemodynamic effects (decreased mean arterial pressure) and beneficial anti-fibrotic effect that are expected to be beneficial, but paradoxically induced cardiac remodeling due to sympathetic activation as recently confirmed [1-5]. As consequences, chronic BNP promoted Ca^{2+} signaling defects and pro-arrhythmogenic effects even in healthy mice.[1] In addition, as in clinics, the dose was chosen to rise circulating BNP level in heart failure individuals who have already high circulating BNP concentration. We already described that supplementation with 0.03 $\mu g.kg^{-1}.min^{-1}$ allows a clear rise in BNP-Sham mice.[1] Thus, we kept 0.03 $\mu g.kg^{-1}.min^{-1}$ to promote a clear rise of circulating BNP level following pump implantation in PMI mice. Thus, BNP level in PMI mice rised slowly during the 2 weeks after the ligation (day-4 after PMI; 0.96 ±0.64 ng/ml n=6, and day-8; 2.26 ±1.79 ng/ml, n=5) and reached steady-state at 3 and 4 weeks after ligature (5.40±1.20 ng/ml and 5.10±0.90 ng/ml, n=7; respectively). At the end of supplementation, circulating BNP levels increased to 11.2±0.7 ng/ml in BNP-PMI, and 11.9±1.0 ng/ml in BB-BNP-PMI mice (n=8 per group) confirming the proper release of product. To note, BNP levels in Shams were inferior to 0.34 ng/ml.

***In vivo* analysis**

Cardiac function was assessed by echocardiography (Vivid7Pro, GE Medical Systems, USA). LV mass, LV shortening fraction, end-diastolic and end-systolic LV dimension were measured.[3] Electrocardiograms were recorded by telemetry (DSI, St. Paul, MN).[3] We have taken care to respect

the Lambeth conventions from the housing of animal to the determination of arrhythmic events.[4] ECG signals were digitally filtered between 0.1 and 1,000 Hz. Heart rate variability, PR, QRS, corrected QT (QTc) intervals and spontaneous arrhythmias were analyzed using 12h nocturnal ECGs (ECG-auto, EMKA Technologies, France).[5] The QT interval was defined as the time between the first deviation from an isoelectric PR interval until the return of the ventricular repolarization to the isoelectric TP baseline from lead II ECGs. The QT correction was performed with the adapted Bazett's formula of Mitchell.[6] To assess the variability of the ventricular repolarization (an index of proarrhythmic outcome), we evaluated the QT interval variability.[7] The mean orthogonal distance from diagonal to the points of the Poincaré plots was calculated and referred to as short term variability of QT (QT_{STV}) by using the formula $QT_{STV}=\sum|QT_n-QT_{n-1}|/(50\times\sqrt{2})$.[8, 9] Only sinus beats were included in the analysis (60 analyses of 1 min every 2 minutes/ 2hours ≈ 40,000 analyzed QRST complexes). To test arrhythmogenic susceptibility, the β-adrenergic catecholamine agonist isoproterenol (2.5 $mg.kg^{-1}$ i.p) was injected just before the end and 4 weeks after the treatment (8 weeks after the ligation). The triggering of sustained ventricular tachycardia (SVT), as defined by the Lambeth conventions (more than 20 successive irregular beats), was monitored. At the same time-points that test of arrhythmogenic susceptibility, blood pressure (systolic, diastolic, mean arterial pressure, in mmHg) was measured non-invasively with a tail cuff and pulse transducer (ML125/M NIBP System, ADInstruments, United-Kingdom). Measurements were performed in triplicate in conscious restrained mice after an acclimatization period of 3 weeks.

Autopsy and heart excision

After euthanasia, autopsies were performed to verify for the presence of pleural effusion. The heart and lungs were excised and weighed, and the heart weight index determined (heart weight/body weight). Lung congestion was established when the lung weight exceeded the mean lung weight of WT animals ± 2 SD.[5] Interstitial fibrosis was measured in 10 μm thick transverse sections of mouse hearts in the peri-infarcted area (Hematoxylin-eosin and Sirius red staining). Results show the area of Sirius red-stained tissue (percentage of total area of myocardial tissue).

RNA extraction and RT-qPCR

Total RNA was extracted from approximately 15-25 mg of left ventricular cardiac tissue, using TRIzol reagent according to the manufacturer's protocol (Euromedex), then treated with DNase I (Invitrogen) at 37°C for 30 min. cDNA was synthesized using superscript II reverse transcriptase (Invitrogen) at 42°C for 50 min. RT-QPCR was performed in duplicates using a LightCycler rapid thermal cycler (Roche, France). Twenty -microliter reaction mixture contained 10 µl of ABsolute QPCR SYBR Green Capillary Mix (Thermo Fisher Scientific, containing thermo start DNA polymerase, reaction buffer, deoxynucleoside trisphosphate mix, 3 mM MgCl2 and SYBR Green I dye), was added with 0.5 µM of appropriate primer mix, and 5 µl of cDNA. Forward and reverse primers for each gene were chosen on the basis of previously published sequences (myocardin-related transcription factor A (MRTF-A) - forward/reverse; CGTGCTCAATGCCTTC/GGCGGATCATTCACTCT; serum response factor (SRF) - forward/reverse TTGTCCCAGCCTGGTTCTCCA/ATCTGCTGAAATCTCTCCACTCTG, NCX1: forward primer aggcggcttctcttttac / reverse primer caacttccaaaaccagag, SERCA2: forward primer agttcatccgctacctcatctca / reverse primer caccagattgacccagagtaactg, S100A1: forward primer cccttctgtcgagaatctgttc / tcagcttatatttgtccccttcc). The amplification program included the initial denaturation step at 95°C for 15 min, and 40 cycles of denaturation at 95°C for 1 s, annealing at 65°C for 10 s, and extension at 72°C for 20 s. Melting curves were used to determine the specificity of PCR products. Data were normalized to GAPDH (8 mice per group).

Ca^{2+} handling

Ca^{2+} experiments were performed on freshly isolated LV myocytes. The mouse was euthanized by cervical dislocation, after which the heart rapidly was excised and retrogradely perfused (Langendorff perfusion) at 37°C for 6–8 min with a modified tyrode solution [113 mM NaCl, 4.7 mM, KCL, 0.6 mM KH2PO4, 0.6 mM Na2HPO4, 1.2 mM MgSO4, 12 mM NaHCO3, 10 mM KHCO3, 10 mM Hepes, 30 mM Taurine (pH 7.4)] containing 0.1g.ml^{-1} Liberase Dispase High Research Grade (Roche, France) perfusion. Cells were kept in 1.8 mM Ca^{2+} (20-22°C) before starting experiments. There was

no difference between age groups. To monitor intracellular Ca^{2+} concentration, cardiomyocytes were loaded with the fluorescent ratiometric Ca^{2+} indicator Indo-1AM (10 µM, *Invitrogen*, France). Cells were field-stimulated at 1.0 Hz with 1-ms current pulses delivered via two platinum electrodes, one on each side of the perfusion chamber (IonOptix system, Hilton, USA) (20V, 1 ms) and simultaneously illuminated at 305 nm using a xenon arc bulb light.[3] Indo-1AM fluorescence emitted at 405 nm and 480nm was recorded simultaneously and Ca^{2+} fluorescence was measured during a 30s pacing period (1.0Hz), followed by a 30s rest period. Diastolic Ca^{2+} levels and the number of cells developing spontaneous irregular Ca^{2+} waves were quantified during the rest period.[3] Ca^{2+} concentration was estimated through the fluorescence ratio (F405/F480). Ca^{2+} transient decay time (t) was measured by fitting the descending phase of the fluorescence trace to a single exponential function. Ca^{2+} sparks were recorded in quiescent cells incubated with Fluo-4AM (5µM, 1.5ms/line; LSM510 Zeiss confocal microscope, 63X water-immersion objective, NA: 1.2) at 25°C.[3] Fluorescence was excited at 488 nm and emission was collected through a 505-nm (F505) long-pass filter. Frequency, averaged amplitude, the full width at half-maximum (FWHM) and full duration at half maximum (FDHM) were measured by following variations of fluorescence at 505nm (ΔF) divided by initial F505 (F0).Cell volume was estimated using Z-stack (x-y projection, front view) image acquisition.[2] Data were analyzed using *ImageJ* and *SparkMaster*.

Ca^{2+} handling proteins

LV were homogenized directly into lysis buffer (20 mM HEPES pH7.4, 40 mM KCl, 1 mM DTT, 0.3% CHAPS, 1 mM PMSF, 1µg/mL leupeptin, 1 µg/mL pepstatin, 1 mM EDTA). Lysates were centrifugated at 6,000 x g for 5 min. Proteins were quantified with DC Protein Assay (Biorad). Fifty micrograms of total proteins were loaded on SDS-PAGE. Proteins were transferred on nitrocellulose membrane (0.2 µm) (GE Healthcare). The membranes were blocked (Blocking buffer from Thermoscientific) and then incubated with primary antibody at 4°C overnight: the sarcoplasmic reticulum Ca^{2+}-ATPase SERCA2a (1:5,000) (A010-20, Badrilla), the Na^{+}-Ca^{2+} exchanger NCX1 (1:1,000) (R3F1, Swant), the ryanodine receptor RyR2 (1:1,000) (Covalab, France), its phosphorylated form, PhosphoSer2808-RyR-2 (1:1,000) (A010-30, Badrilla, UK), phospholamban (1:20,000) (A010-

14, Badrilla) and its phosphorylated form PhosphoSer16-PLB (1:5,000) (A010-12, Badrilla) and the Ca^{2+}-binding protein S100A1 (1:2,500) (SP5355P, Acris antibodies GmbH, Germany). Protein levels were expressed relative to GAPDH (1:60,000) (ab8245, Abcam, France). The membranes were then incubated with secondary antibody: anti-rabbit 800 nm (1:30,000) (for SERCA2a, PhosphoPLB, RyR2, PhosphoRyR2 and S100A1) or anti-mouse 800 nm (1:30,000) (for NCX1, PLB and GAPDH) for 1h in the dark. After the final washes, the membranes were scanned by using Odyssey Infrared Imager (LI-COR Biosciences).

Cellular electrophysiology

Whole-cell voltage- and current-clamp experiments were performed at room temperature on rod-shaped Ca^{2+}-tolerant myocytes using whole-cell patch-clamp techniques (22-24°C), with an Axopatch 1D amplifier interfaced through a microcomputer equipped with a Digidata 1200 digitizer and pClamp 8 software (Axon Instruments). For voltage- and current-clamp experiments, the recording pipettes contained (in mmol/L): KCl 120; EGTA 11; HEPES 10; $MgCl_2$ 6.8; $CaCl_2$ 4.7 $ATPNa_2$ 4 and $GTPNa_2$ 0.4 (pH 7.2). The bath solution contained (in mmol/L): NaCl 130; KCl 4; MgCl2 1.8; CaCl2 1.8; HEPES 10; glucose 11; CoCl2 5 and tetrodotoxin (TTX) 0.02 (pH 7.4). Whole-cell membrane capacitance and series resistance in each cell were measured and compensated electronically (>80%) prior to recording membrane currents. Whole-cell voltage-gated outward K^+ currents were evoked by 4.5 s voltage steps to potentials between –40 and +50 mV from a holding potential (HP) of –80 mV. The inward rectifying current, referred to as I_{K1}, was recorded by applying 450 ms voltage steps to potentials between -120 and -40 mV from a HP of -80 mV. For ICa,L study, external recording solution contained 136 mM tetraethylammonium (TEA)-Cl, 2 mM $CaCl_2$, 1.8 mM $MgCl_2$, 10 mM Hepes, 5 mM 4-aminopyridine, and 10 mM glucose, pH 7.4, with TEA-OH. Pipette solution contained 125 mM CsCl, 20 mM TEA-Cl, 10 mM EGTA, 10 mM Hepes, 5 mM phosphocreatine, 5 mM Mg_2-ATP, and 0.3 GTP, pH 7.2, with CsOH. Myocytes were held at –80 mV, and 10-mV depolarizing steps from –50 to 50 mV for 300 ms were applied. For current-clamp experiments, TTX and CoCl2 were omitted from the bath solution, and action potentials (APs) were recorded in response to brief (1-

2 ms) depolarizing current injections delivered at 1 Hz. Voltage-clamp data were analyzed using Clampfit (Axon Instruments, UK). Integration of the capacitive transients recorded during brief ±10 mV voltage steps from the HP provided whole-cell membrane capacitances (Cm). Leak currents (<10 pA) were not corrected. Peak currents at each test potential were defined as the maximal outward K^+ current. The amplitudes and time constants of inactivation (τ_{inact}) of $I_{to,f}$, $I_{K,slow}$ and I_{ss} were determined from double exponential fits to the decay phases of the outward K^+ currents, as described [1]. Current amplitudes were normalized to whole-cell membrane capacitance, and current densities (pA/pF) reported. The resting membrane potential, and the amplitude and duration of AP at 20% (APD_{20}), 50% (APD50) and 90% (APD90) repolarization were also measured."

Statistical analysis

All data are reported as means±SD (mean±SE for patch-clamp experiments). Statistical analyses were performed using GraphPad Prism and Origin Softwares. One-way ANOVA for multiple comparisons was used, followed by a parametric t-test with Bonferroni's correction. Percentage data were analyzed by a *chi-square* test. A p-value of 0.05 or less indicated a statistically significant difference.

Calcium leak in heart failure

To date, what known about Ca^{2+} cycling in healthy and heart failure conditions?

Ca^{2+}-induced Ca^{2+} release (CICR) is the basis of cardiac excitation-contraction coupling. During systole, the L-type Ca^{2+} channels (LTCC) activate type-2 ryanodine receptors (RYR2), which release Ca^{2+} from sarcoplasmic reticulum (SR).[2] After CICR, cytosolic Ca^{2+} is mainly re-uptaken by the SERCA2a into SR, thereby leading to relaxation during diastole. During diastole, simultaneous spontaneous activations of RyR2 generate local increase in cytosolic Ca^{2+}, events named as Ca^{2+} sparks.[3] These sparks are mostly responsible for the diastolic SR Ca^{2+} leak in ventricular cardiomyocytes.[4-6]

In healthy conditions, the RyR2 can spontaneously open and induce SR Ca^{2+} leak during diastole, a phenomenon that participates to the regulation of SR Ca^{2+} load.[6]

During heart failure, ventricular cardiomyocytes exhibit a down regulation of SERCA2a activity leading to a slower decay of cytosolic Ca^{2+} transient and consecutive impairment of Ca^{2+} reuptake into the SR.[7] As a result, cytosolic Ca^{2+} level in end-diastole increases and a prolongation of the Ca^{2+} transient occurs in heart failure.[8, 9] In parallel, failing cardiomyocytes present increased expression and activity of Na^{+}/Ca^{2+} exchanger (NCX).[10, 11] Thus, SR Ca^{2+} efflux in diastole can influence cardiac function by depleting the SR Ca^{2+} content. Moreover, increased Ca^{2+} leak (Ca^{2+} sparks) is observed in several models of heart failure, which contributes to increase cytosolic Ca^{2+} level in diastole.[12, 13] This Ca^{2+} leak is implicated in the reduction of contractile force by reducing the SR Ca^{2+} load and can also be pro-arrhythmogenic through the extrusion of Ca^{2+} by the electrogenic NCX.[14, 15]. Associated with the electrogenic activity of NCX, the summation of Ca^{2+} released from several local sparks could trigger CICR and generate arrhythmogenic spontaneous Ca^{2+} waves, independently of Ca^{2+} entry via the LTCC.[4, 16]

Shannon et al addressed how SR Ca^{2+} load could modify SR Ca^{2+} leak and conversely.[6] They determined that : (1) SR Ca^{2+} load depends both on Ca^{2+} leak from RyR2 and Ca^{2+} gradient through the SR Ca^{2+} ATPase, and (2) Ca^{2+} leak, even in healthy animals, has measurable effect on SR Ca^{2+} load. In addition, they showed that SR Ca^{2+} load regulates the Ca^{2+} leak (*i.e.* a load dependence of the leak). They observed that SR Ca^{2+} leak increases with SR Ca^{2+} load in intact *healthy cardiomyocytes*, i.e. without any modification (expression or post-traductional modifications) of key Ca^{2+} handling proteins (SERCA2a, NCX, and S100A1.[6] To summarize, in healthy conditions, at higher cytosolic Ca^{2+} in diastole, the higher Ca^{2+} leak prevents a deleterious SR Ca^{2+} overload. As SR Ca^{2+} load increases, the Ca^{2+} leak increases. As Ca^{2+} leak increases, the SR Ca^{2+} load decreases.[6] In addition, these authors argued that anything that could shift the relationship between SR Ca^{2+} load or RyR opening (as modification of Ca^{2+} handling protein expression or activity due do modification of expressions or post-traductional modifications) could change the SR Ca^{2+} load for a given cytoplasmic diastolic Ca^{2+} level.[6] Reciprocally, SR Ca^{2+} leak increases for a given SR Ca^{2+} load.[17] Thus, in

heart failure conditions, with major modifications of activity of Ca^{2+} handling protein, Shannon at al. suggested that if SR Ca^{2+} leak is increased in heart failure, it may reduce SR Ca^{2+} load and SR Ca^{2+} release in diastole as they previously observed.[18, 19] This concept was also developed by Marx and collaborators (see [20] for review) i.e. ; a high persistent diastolic SR Ca^{2+} leak due to increased Ca^{2+} sparks frequency is responsible for excitation-contraction coupling defect in heart failure. Associated with increased NCX activity and reduced Ca^{2+} reuptake into SR by SERCA2a that decreased SR Ca^{2+} load, this high Ca^{2+} sparks frequency induces spontaneous CICR and is responsible for spontaneous Ca^{2+} waves and arrhythmia. In brief, the SR Ca^{2+} leak conversely influences the SR Ca^{2+} load in diastole and reduces the SR Ca^{2+} release during systole.[6, 18, 19]

This theory is largely supported by literature. Indeed, the level of cytosolic Ca^{2+} also regulates the SR Ca^{2+} leak directly by binding to the high-affinity activation site of the cytosolic side of the RyR.[21] These results were elegantly confirmed by Bovo et collaborators who directly measured SR Ca^{2+} leak as the rate of SR Ca^{2+} declines after SERCA inhibition in both healthy (that could exaggeratedly mimic the decrease of SERCA2a activity during heart failure) and in failing cardiomyocytes.[12, 22] As elevated SR Ca^{2+} declines and low cytosolic Ca^{2+} level in diastole rises, Ca^{2+} leak, as Ca^{2+} sparks frequency, increases. This is sufficient to trigger spontaneous pro-arrhythmogenic Ca^{2+} waves.[22]

Ca^{2+} Sparks "morphology" also brings valuable information about spontaneous Ca^{2+} release and physiological regulation of this process.[3] Thus, the amplitude of Ca^{2+} sparks proportionally decreases with the reduction of SR Ca^{2+} load and the augmentation of cytosolic Ca^{2+} level in diastole.[22] In the same way, the spatial width of a spark, usually represented by the full width at half-maximum (FWHM) and the full duration at half maximum (FDHM) revealing parameters of microscopic Ca^{2+} diffusion and reaction, could reflect modification of RyR activity independent to SR Ca^{2+} load.[3, 23]

Comparing Ca^{2+} leak theory and previous works with our results.

Our experimental results are consistent with this theory and expected results in PMI mice. Indeed, in PMI, we observed that Ca^{2+} uptake by the SR, mainly regulated by the activity of SERCA2a and its

regulatory proteins PLB [24], was impaired as revealed by the reduced Ca^{2+} transient decay rate that leads to subsequent increase in diastolic cytosolic Ca^{2+}. The increase in Ca^{2+} level in diastole promoted a persistent SR Ca^{2+} leak (higher Ca^{2+} sparks frequency) and conversely influenced the SR Ca^{2+} load which was proportionally decreased. All our results conformed with the results of Bers, Bovo and co-workers [12, 22] In addition, the higher sparks frequency, expected to promote spontaneous Ca^{2+} waves, increased the number of cardiomyocytes triggering abnormal spontaneous Ca^{2+} waves. The decrease in SR Ca^{2+} content and lower Ca^{2+} transient amplitude accounted for the decrease of cellular contraction. In addition, as expected, the amplitude of Ca^{2+} sparks was decreased in cardiomyocytes isolated from PMI mice according to decreased SR Ca^{2+} content (See new figure 4).[22] The full width at half-maximum (FWHM) and the full duration at half maximum (FDHM) were also increased in PMI animal. Other authors also found increase in FWHM and FDHM when cytosolic Ca^{2+} was increased (See figure 4).[23, 25-28]

Thus, in our model, an increase in Ca^{2+} spark frequency could result from an increase in cytosolic Ca^{2+} level due to blunted SERCA2a activity, associated with a modulation of the intrinsic properties of the RyR2 complex. This decreased SR Ca^{2+} load as we observed after caffeine application in PMI mice. In BNP-PMI mice, the further reduction of S100A1 when compared to PMI could account for the worsening of Ca^{2+} signaling and further increase in Ca^{2+} leak and reduction of SR Ca^{2+} content. Indeed, the decrease of S100A1 reported in HF[29] promotes SR Ca^{2+} leak via RyR2 increased open probability,[30] and decreases Ca^{2+} re-uptake via the SERCA2a.[29] As consequences, RyR2 characteristics (frequency, amplitude, FWHM, and FDHM) were further altered [30](Figure 4) without modification of Ser 16 phosphorylation by PKA. Of note, decreased S100A1 also induces prolonged ventricular repolarization in response to sympathetic activation as observed by others in HF [31] and also in our experiments.

Thus, our results are in line with the more recent theory to treat heart failure by targeting –first, the down-regulation of SERCA2a activity, secondly the aberrant RyR2 opening in diastole,[32] and –third, the decreased expression of the Ca^{2+} handling protein S100A1; an endogenous regulator of both SERCA2a and RyR2 function.[33] To note, S100A1 was more efficient when added to β-blocker.[34]

Mechanism of pro-arrhythmogenic effect of BNP

We used the patch-clamp technique to measure the action potential with a current-clamp approach, and the depolarizing $I_{Ca,L}$ and repolarizing K^+ current I_K (I_{t0}, I_{Kslow} and $I_{ss,\ k1}$) in voltage-clamp conditions in BNP-PMI, PMI and Sham mice. We observed that PMI mice present an increase in AP duration when compared to Sham animals, as already described.[35], with a lengthening of APD50 and APD90 (Figure *S5*, Table *S1*). The LV cardiomyocytes isolated from PMI mice also exhibited a significant reduction of $I_{Ca,L}$ current density (when compared with shams) as already described.[36, 37] The steady-state inactivation was also right-shifted to more positive potentials and $I_{Ca,L}$ decay kinetics were dramatically slowed in line with high cytosolic Ca^{2+} in diastole. All results conformed to literature.[38]

The inwardly rectifying I_{K1} current was not significantly altered in our model. Data in literature diverged on change in the inward rectifying current in disease hearts. In rat failing cardiomyocytes, I_{K1} was found to be reduced,[39] whereas in spontaneous hypertensive rats, in failing rabbit and in aorta-constricted guinea-pig, it was unchanged.[40-42] In myocytes isolated from human or dog failing left ventricle, I_{K1} was slightly decreased, however, difference was found at potential that do not contribute to AP repolarisation.[43, 44] In contrast to I_{K1}, we showed a diminution of the outwardly rectifying potassium currents (I_{to}, I_{Kslow}**)** in PMI mice compared with sham animal as already described.[45] We obtained results comparable with that of Tsuji *et al.*[46] In addition, early afterdepolarizations (EAD) were observed in 20% of LV cardiomyocytes of PMI mice during repetitive stimulation, while cardiomyocytes isolated from sham mice did not develop these EADs.

BNP had no further effect on AP duration, K^+ and Ca^{2+} current density and inactivation of PMI animal (BNP-PMI group). However, BNP treatment strongly increased the occurrence of EAD in LV cell from BNP-PMI mice (54% of cells).

While membrane potential of PMI cells presented a slight depolarization when compared to sham cell, BNP induced a net depolarization of the resting membrane potential in BNP-PMI mice, a phenomenon already described in non cardiac cell.[47] In addition, at APD50 and APD90, the membrane potential

was more positive in BNP-PMI when compared to PMI animal. Interestingly, Nifedipine blocked all EADs in both PMI and BNP-PMI animal, suggesting the implication of Ca^{2+}-dependent mechanism.

Both early and delayed afterdepolarizations have been incriminated in the generation of cardiac arrhythmia in failing patients. In fact, the progression and severity of left ventricular dysfunction may generate two distinct mechanisms of ventricular arrhythmia.[48, 49] The cellular mechanism relies on oscillations of cellular membrane potential referred as early (EAD) or delayed (DAD) afterdepolarizations. In healthy conditions, the large repolarizing I_{to} current prevents abnormal repolarization and limits trans-sarcolemna Ca^{2+} influx via I_{Cal} and, thereby, propensity for EADs during the AP plateau.[39, 50] The blunting of I_{to} in PMI in combination with the frequency-dependent enhancement of $I_{Ca,L}$ sets two important conditions for the occurrence of EADs. The electrogenic NCX is also incriminated in EAD triggering.[51] Indeed, as pointed by Sipido et al., when NCX is inward during the low AP plateau, the exchange current might prolong the AP duration and set the stage for EAD and, conversely, when AP was lengthened, the inward current generated by NCX during the AP plateau could be enhanced.[11, 52] Thus, high cytosolic Ca^{2+} level in HF could maximize this electrogenic effect and favors a membrane potential depolarization. Indeed, since membrane potential varies faster than E_{NaCa} during CICR and since the membrane potential Em is more negative than E_{NaCa} during the low plateau of the AP, the NCX in normal mode generates an inward current.[53] This was firstly theorized by Mullins in 1981 (Mullins LJ. Ion Transport in the Heart. New York: Raven Press, 1981) and nicely reviewed by Janvier and Boyett.[53]

In addition, abnormal spontaneous cytosolic Ca^{2+} waves can also influence arrhythmogenesis by promoting, sudden repolarization change and EADS.[54] In this way, several authors showed that aftercontraction and Ca^{2+} waves could precede the up-stroke of EAD that supports the role of SR Ca^{2+} release and indicates the involvement of a Ca^{2+}-dependent current. The smaller Ca^{2+} transient in HF may also cause less complete inactivation of $I_{Ca,L}$ during the early phases of AP and participate to increase the likehood of reactivation of inward $I_{Ca,L}$ *late* during the AP, which favors EAD triggering.[55, 56] This dynamic regulation of $I_{Ca,L}$ and NCX by SR-Ca^{2+} release and high cytosolic

Ca^{2+} plays an important role in triggering EAD which might be amplified during chronic sympathetic overdrive.[57, 58] Thus it has been proposed that EAD is the result of Ca^{2+}-induced Ca^{2+} release, enhanced electrogenic activity of NCX due to high cytosolic Ca^{2+} in diastole and sarcolemnal "windows $I_{Ca,L}$ current favored by reduced systolic Ca^{2+} transient.[59] As a confirmation of this theory, Ca^{2+} current blocker nifedipine prevented all EAD,[51] as we also showed.

In conclusion, our data compared with those of the literature suggest that, in PMI mice, the modification of the electrophysiological properties of ventricular cardiomyocytes including diminished repolarizing K^+ current and decreased slow $I_{Ca,L}$ inactivation accounting for the lengthened AP repolarization, associated with high cytosolic Ca^{2+} level due to Ca^{2+} leak in diastole from SR, reduced Ca^{2+} transient amplitude in systole and increased expression of NCX, could be responsible for the triggering of EADs. These EAD, known to induce dispersion of repolarization which favors reentry,[60] modified the variability of QT (ventricular repolarization) as in our PMI mice which are more prone to trigger spontaneous and catecholamines-induced ventricular arrhythmia than Sham animals.

In BNP-PMI mice, the electrophysiological properties ($I_{Ca,L}$, I_K) were not further modified when compared to that of PMI animal. So, we focused on the Ca^{2+} signaling since the only difference was an increase of Ca^{2+} leak via RyR2 in diastole which decreased SR-Ca^{2+} content, an increased cytosolic Ca^{2+} in diastole, and a reduced Ca^{2+} transient in systole. By comparing with the literature, this could accounted for by an increase of inward electrogenic NCX activity and more depolarized membrane potential as seen at APD50 and APD90, and therefore for the higher propensity to trigger EAD than in PMI animals. As consequences, BNP-PMI mice exhibited high QT repolarization variability than PMI mice and presented higher occurrence of ventricular extrasystoles, tachycardia and fibrillation leading to cardiac death after β-agonist injection. Approaches that could improve Ca^{2+} signaling (reduced Ca^{2+} leak in diastole and increase systolic Ca^{2+} transient, normalization of Ca^{2+}-handling protein expression or activity) could thus diminish the pro-arrhythmogenicity as we showed with the BB-BNP combination.

References

1 Brunet S, Aimond F, Li H, et al. Heterogeneous expression of repolarizing, voltage-gated K+ currents in adult mouse ventricles. *J Physiol* 2004;**559**:103-20.

2 Fabiato A. Calcium-induced release of calcium from the cardiac sarcoplasmic reticulum. *Am J Physiol* 1983;**245**:C1-14.

3 Cheng H, Lederer WJ. Calcium sparks. *Physiol Rev* 2008;**88**:1491-545.

4 Cheng H, Lederer WJ, Cannell MB. Calcium sparks: elementary events underlying excitation-contraction coupling in heart muscle. *Science* 1993;**262**:740-4.

5 Bassani RA, Bers DM. Rate of diastolic Ca release from the sarcoplasmic reticulum of intact rabbit and rat ventricular myocytes. *Biophys J* 1995;**68**:2015-22.

6 Shannon TR, Ginsburg KS, Bers DM. Quantitative assessment of the SR Ca2+ leak-load relationship. *Circ Res* 2002;**91**:594-600.

7 Mercadier JJ, Lompre AM, Duc P, et al. Altered sarcoplasmic reticulum Ca2(+)-ATPase gene expression in the human ventricle during end-stage heart failure. *J Clin Invest* 1990;**85**:305-9.

8 Morgan JP. Abnormal intracellular modulation of calcium as a major cause of cardiac contractile dysfunction. *N Engl J Med* 1991;**325**:625-32.

9 Lindner M, Erdmann E, Beuckelmann DJ. Calcium content of the sarcoplasmic reticulum in isolated ventricular myocytes from patients with terminal heart failure. *J Mol Cell Cardiol* 1998;**30**:743-9.

10 Hasenfuss G, Schillinger W, Lehnart SE, et al. Relationship between Na+-Ca2+-exchanger protein levels and diastolic function of failing human myocardium. *Circulation* 1999;**99**:641-8.

11 Sipido KR, Volders PG, Vos MA, et al. Altered Na/Ca exchange activity in cardiac hypertrophy and heart failure: a new target for therapy? *Cardiovasc Res* 2002;**53**:782-805.

12 Zima AV, Bovo E, Bers DM, et al. Ca(2)+ spark-dependent and -independent sarcoplasmic reticulum Ca(2)+ leak in normal and failing rabbit ventricular myocytes. *J Physiol* 2010;**588**:4743-57.

13 Thireau J, Karam S, Fauconnier J, et al. Functional evidence for an active role of B-type natriuretic peptide in cardiac remodelling and pro-arrhythmogenicity. *Cardiovasc Res* 2012;**95**:59-68.

14 Kass RS, Lederer WJ, Tsien RW, et al. Role of calcium ions in transient inward currents and aftercontractions induced by strophanthidin in cardiac Purkinje fibres. *J Physiol* 1978;**281**:187-208.

15 George CH. Sarcoplasmic reticulum Ca2+ leak in heart failure: mere observation or functional relevance? *Cardiovasc Res* 2008;**77**:302-14.

16 Diaz ME, Trafford AW, O'Neill SC, et al. Measurement of sarcoplasmic reticulum Ca2+ content and sarcolemmal Ca2+ fluxes in isolated rat ventricular myocytes during spontaneous Ca2+ release. *J Physiol* 1997;**501 (Pt 1)**:3-16.

17 Bers DM. Cardiac Sarcoplasmic Reticulum Calcium Leak: Basis and Roles in Cardiac Dysfunction. *Annu Rev Physiol* 2013.

18 Shannon TR, Ginsburg KS, Bers DM. Potentiation of fractional sarcoplasmic reticulum calcium release by total and free intra-sarcoplasmic reticulum calcium concentration. *Biophys J* 2000;**78**:334-43.

19 Bassani JW, Yuan W, Bers DM. Fractional SR Ca release is regulated by trigger Ca and SR Ca content in cardiac myocytes. *Am J Physiol* 1995;**268**:C1313-9.

20 Marx SO, Marks AR. Dysfunctional ryanodine receptors in the heart: new insights into complex cardiovascular diseases. *J Mol Cell Cardiol* 2013;**58**:225-31.

21 Rousseau E, Smith JS, Henderson JS, et al. Single channel and 45Ca2+ flux measurements of the cardiac sarcoplasmic reticulum calcium channel. *Biophys J* 1986;**50**:1009-14.

22 Bovo E, Mazurek SR, Blatter LA, et al. Regulation of sarcoplasmic reticulum Ca(2)(+) leak by cytosolic Ca(2)(+) in rabbit ventricular myocytes. *J Physiol* 2011;**589**:6039-50.

23 Gomez AM, Rueda A, Sainte-Marie Y, et al. Mineralocorticoid modulation of cardiac ryanodine receptor activity is associated with downregulation of FK506-binding proteins. *Circulation* 2009;**119**:2179-87.

24 Ikeda Y, Hoshijima M, Chien KR. Toward biologically targeted therapy of calcium cycling defects in heart failure. *Physiology (Bethesda)* 2008;**23**:6-16.

25 Song LS, Pi Y, Kim SJ, et al. Paradoxical cellular Ca2+ signaling in severe but compensated canine left ventricular hypertrophy. *Circ Res* 2005;**97**:457-64.

26 Zhang GQ, Wei H, Lu J, et al. Identification and characterization of calcium sparks in cardiomyocytes derived from human induced pluripotent stem cells. *PLoS One* 2013;**8**:e55266.

27 Lukyanenko V, Gyorke S. Ca2+ sparks and Ca2+ waves in saponin-permeabilized rat ventricular myocytes. *J Physiol* 1999;**521 Pt 3**:575-85.

28 Xiao RP, Valdivia HH, Bogdanov K, et al. The immunophilin FK506-binding protein modulates Ca2+ release channel closure in rat heart. *J Physiol* 1997;**500 (Pt 2)**:343-54.

29 Most P, Pleger ST, Volkers M, et al. Cardiac adenoviral S100A1 gene delivery rescues failing myocardium. *J Clin Invest* 2004;**114**:1550-63.

30 Volkers M, Loughrey CM, Macquaide N, et al. S100A1 decreases calcium spark frequency and alters their spatial characteristics in permeabilized adult ventricular cardiomyocytes. *Cell Calcium* 2007;**41**:135-43.

31 Ackermann GE, Domenighetti AA, Deten A, et al. S100A1 deficiency results in prolonged ventricular repolarization in response to sympathetic activation. *Gen Physiol Biophys* 2008;**27**:127-42.

32 Marks AR. Calcium cycling proteins and heart failure: mechanisms and therapeutics. *J Clin Invest* 2013;**123**:46-52.

33 Brinks H, Rohde D, Voelkers M, et al. S100A1 genetically targeted therapy reverses dysfunction of human failing cardiomyocytes. *J Am Coll Cardiol* 2011;**58**:966-73.

34 Pleger ST, Most P, Boucher M, et al. Stable myocardial-specific AAV6-S100A1 gene therapy results in chronic functional heart failure rescue. *Circulation* 2007;**115**:2506-15.

35 Wickenden AD, Kaprielian R, Kassiri Z, et al. The role of action potential prolongation and altered intracellular calcium handling in the pathogenesis of heart failure. *Cardiovasc Res* 1998;**37**:312-23.

36 Aimond F, Alvarez JL, Rauzier JM, et al. Ionic basis of ventricular arrhythmias in remodeled rat heart during long-term myocardial infarction. *Cardiovasc Res* 1999;**42**:402-15.

37 Shi CX, Wang YH, Dong F, et al. [Transmural L-type calcium current in a pressure-overloaded mouse model with heart failure]. *Sheng Li Xue Bao* 2007;**59**:19-26.

38 Benitah JP, Alvarez JL, Gomez AM. L-type Ca(2+) current in ventricular cardiomyocytes. *J Mol Cell Cardiol* 2010;**48**:26-36.

39 Fauconnier J, Lacampagne A, Rauzier JM, et al. Ca2+-dependent reduction of IK1 in rat ventricular cells: a novel paradigm for arrhythmia in heart failure? *Cardiovasc Res* 2005;**68**:204-12.

40 Cerbai E, Barbieri M, Li Q, et al. Ionic basis of action potential prolongation of hypertrophied cardiac myocytes isolated from hypertensive rats of different ages. *Cardiovasc Res* 1994;**28**:1180-7.

41 Ryder KO, Bryant SM, Hart G. Membrane current changes in left ventricular myocytes isolated from guinea pigs after abdominal aortic coarctation. *Cardiovasc Res* 1993;**27**:1278-87.

42 Rozanski GJ, Xu Z, Whitney RT, et al. Electrophysiology of rabbit ventricular myocytes following sustained rapid ventricular pacing. *J Mol Cell Cardiol* 1997;**29**:721-32.

43 Beuckelmann DJ, Nabauer M, Erdmann E. Alterations of K+ currents in isolated human ventricular myocytes from patients with terminal heart failure. *Circ Res* 1993;**73**:379-85.

44 Kaab S, Nuss HB, Chiamvimonvat N, et al. Ionic mechanism of action potential prolongation in ventricular myocytes from dogs with pacing-induced heart failure. *Circ Res* 1996;**78**:262-73.

45 Wang Y, Cheng J, Chen G, et al. Remodeling of outward K+ currents in pressure-overload heart failure. *J Cardiovasc Electrophysiol* 2007;**18**:869-75.

46 Tsuji Y, Opthof T, Kamiya K, et al. Pacing-induced heart failure causes a reduction of delayed rectifier potassium currents along with decreases in calcium and transient outward currents in rabbit ventricle. *Cardiovasc Res* 2000;**48**:300-9.

47 Hirsch JR, Meyer M, Magert HJ, et al. cGMP-dependent and -independent inhibition of a K+ conductance by natriuretic peptides: molecular and functional studies in human proximal tubule cells. *J Am Soc Nephrol* 1999;**10**:472-80.

48 Solomon SD, Zelenkofske S, McMurray JJ, et al. Sudden death in patients with myocardial infarction and left ventricular dysfunction, heart failure, or both. *N Engl J Med* 2005;**352**:2581-8.

49 Buxton AE. Sudden death after myocardial infarction--who needs prophylaxis, and when? *N Engl J Med* 2005;**352**:2638-40.

50 Fauconnier J, Bedut S, Le Guennec JY, et al. Ca2+ current-mediated regulation of action potential by pacing rate in rat ventricular myocytes. *Cardiovasc Res* 2003;**57**:670-80.

51 Schouten VJ, ter Keurs HE, Quaegebeur JM. Influence of electrogenic Na/Ca exchange on the action potential in human heart muscle. *Cardiovasc Res* 1990;**24**:758-67.

52 Sipido KR, Volders PG, de Groot SH, et al. Enhanced Ca(2+) release and Na/Ca exchange activity in hypertrophied canine ventricular myocytes: potential link between contractile adaptation and arrhythmogenesis. *Circulation* 2000;**102**:2137-44.

53 Janvier NC, Boyett MR. The role of Na-Ca exchange current in the cardiac action potential. *Cardiovasc Res* 1996;**32**:69-84.

54 Xie LH, Weiss JN. Arrhythmogenic consequences of intracellular calcium waves. *Am J Physiol Heart Circ Physiol* 2009;**297**:H997-H1002.

55 Shorofsky SR, January CT. L- and T-type Ca2+ channels in canine cardiac Purkinje cells. Single-channel demonstration of L-type Ca2+ window current. *Circ Res* 1992;**70**:456-64.

56 Zeng J, Rudy Y. Early afterdepolarizations in cardiac myocytes: mechanism and rate dependence. *Biophys J* 1995;**68**:949-64.

57 Antoons G, Volders PG, Stankovicova T, et al. Window Ca2+ current and its modulation by Ca2+ release in hypertrophied cardiac myocytes from dogs with chronic atrioventricular block. *J Physiol* 2007;**579**:147-60.

58 Richard S, Perrier E, Fauconnier J, et al. 'Ca(2+)-induced Ca(2+) entry' or how the L-type Ca(2+) channel remodels its own signalling pathway in cardiac cells. *Prog Biophys Mol Biol* 2006;**90**:118-35.

59 January CT, Moscucci A. Cellular mechanisms of early afterdepolarizations. *Ann N Y Acad Sci* 1992;**644**:23-32.

60 Volders PG, Kulcsar A, Vos MA, et al. Similarities between early and delayed afterdepolarizations induced by isoproterenol in canine ventricular myocytes. *Cardiovasc Res* 1997;**34**:348-59.

Supplementary Figures

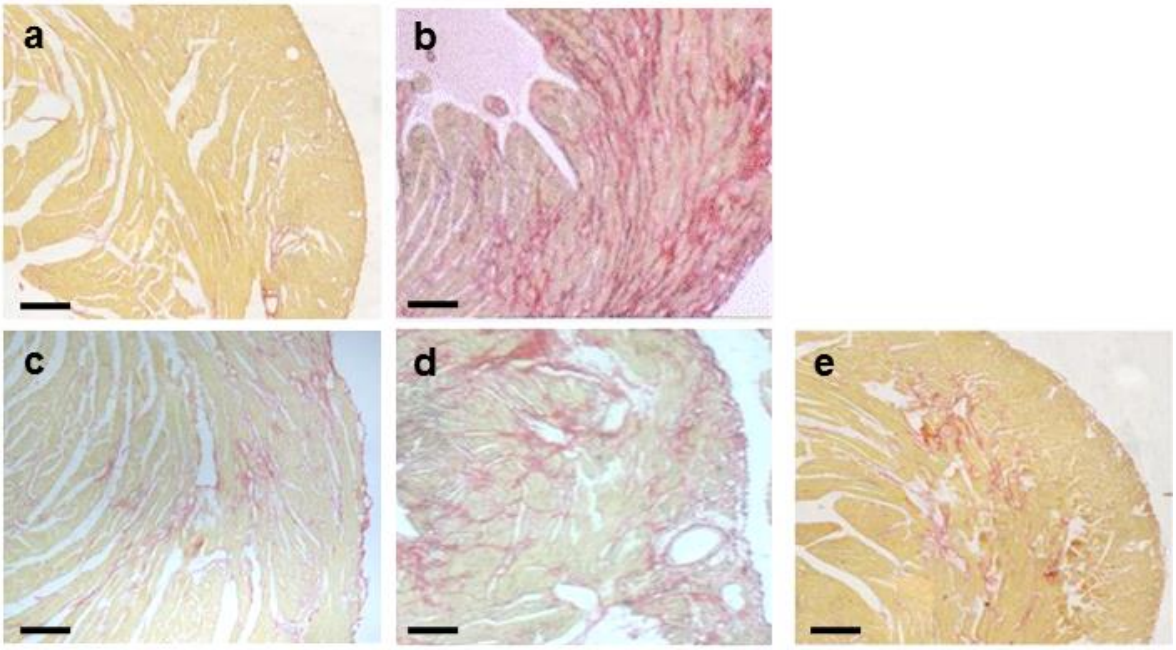

Supplementary Figure S1.
Thireau et al.

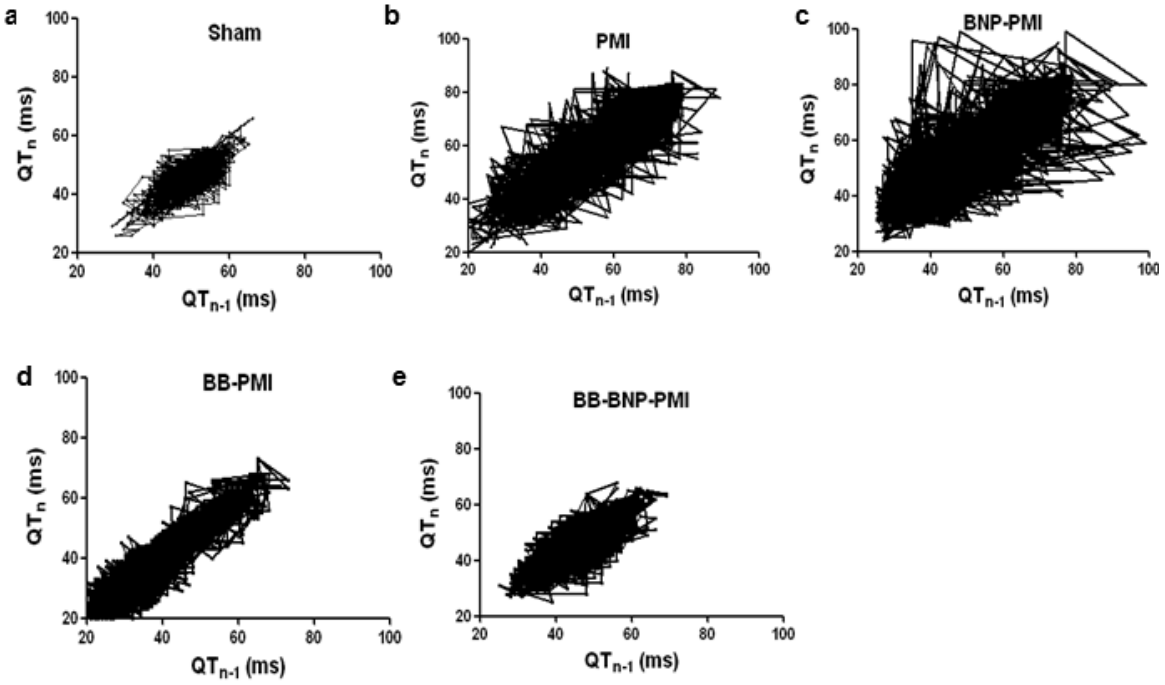

Supplementary Figure S2.
Thireau et al.

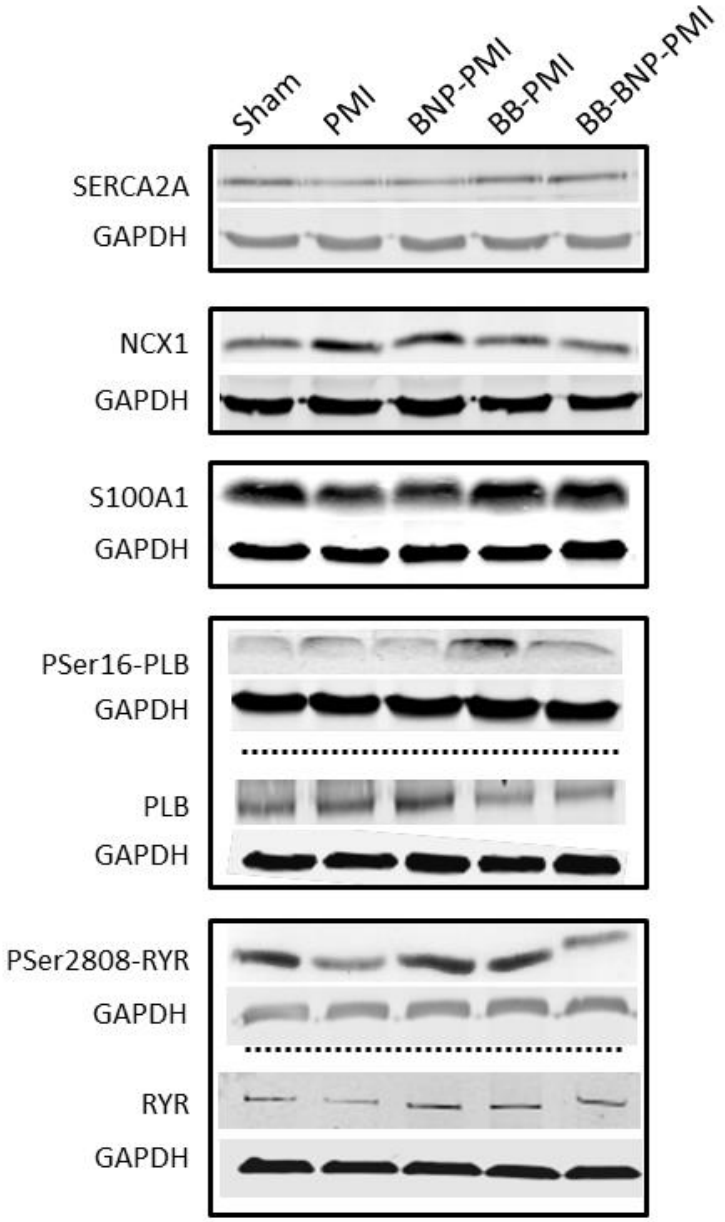

Supplementary Figure S3.
Thireau et al.

Supplementary Table 1. Non-invasive blood pressure measurement

	Sham	PMI	BNP-PMI	BB-PMI	BB-BNP-PMI
Blood pressure during treatment					
Systolic (mmHg)	128.5±5.1	103.4±1.9 ‡	100.1±1.9 ‡	96.3±1.9 ‡	98.6±1.8 ‡
Diastolic (mmHg)	106.9±3.6	97.0±1.8 †	92.1±1.3 ‡,§	88.4±1.8 ‡,§	89.5±1.7 ‡,§
Mean (mmHg)	116.8±3.6	100.2±1.7 †	94.1±1.4 ‡,§	91.4±1.8 ‡,§	92.2±1.9 ‡,§
Blood pressure after treatment					
Systolic (mmHg)	133.7±1.1	101.8±1.8 ‡	111.6±2.8 †,§	103.2±1.5 ‡	119.3±2.7 †,§
Diastolic (mmHg)	107.9±3.6	95.8±3.9 †	102.6±3.3 *,§	94.2±1.1 †	102.5±2.7 *,§
Mean (mmHg)	116.4±2.1	97.1±2.6 ‡	105.6±2.7 *,§	97.3±1,1 ‡	108.0±1.3 *,§

Supplementary Table. S2. mRNA expression of hypertrophic markers and Ca^{2+} handling proteins.

	Sham	PMI	BNP-PMI	BB-PMI	BB-BNP-PMI
MRTF-A	1.48±0.19	3.16±0.14 †	2.58±0.21 *,§	2.36±0.12 *,§	1.42±0.09 ‖,#
SRF	1.77±0.09	2.62±0.27 *	2.41±0.34 *	1.99±0.14 §	1.55±0.16 ‖,#
SERCA2A	1.49±0.16	0.84±0.17 *	0.34±0.20 †,§	1.91±0.14 †,§	2.66±0.16 ‡,‖,#
NCX1	0.82±0.26	1.98±0.24 †	2.3±0.34 †	1.51±0.14 *	0.64±0.26 ‖,#
S100A1	5.96±0.26	3.08±0.24 †	1.67±0.34 ‡,§	4.21±0.14 †	5.33±0.26 §,#

Supplementary Table S3: Action potential and ionic currents characteristics.

	Sham	**PMI**	**PMI-BNP**
Action potential			
Arrhythmia (EAD)	0 event	2 /20 cells	6 /11 cells
RMP (mV) n=	-90.0 ± 1.5 *11*	-79.9 ± 1.3 * *20*	-72.4 ± 0.8 *;£ *11*
Amplitude (mV) n=	127.0 ± 4.7 *11*	123.0 ± 2.5 *20*	119.2 ± 2.8 *11*
APD20 (ms) V_m (mV) n=	1.1 ± 0.1 11.4 ± 3.6 *11*	3.4 ± 0.6 * 18.5 ± 2.4 *20*	2.1 ± 0.3 * 23.0 ± 1.8 * *11*
APD50 (ms) V_m (mV) n=	4.3 ± 1.0 -26.4 ± 2.3 *11*	18.7 ± 3.2 * -18.5 ± 1.8 * *20*	11.8 ± 2.6 * -12.6 ± 1.1 *;£ *11*
APD90 (ms) V_m (mV) n=	29.5 ± 4.0 -77.4 ± 1.4 *11*	99.1 ± 13.3 * -68.3 ± 1.3 * *20*	96.1 ± 22.7 * -61.1 ± 0.9 *;£ *7*
Ionic currents			
$I_{K,peak}$ density (pA/pF) n=	68 ± 8.1 *13*	30.5 ± 3.7 * *22*	30.2 ± 6.5 * *13*
$I_{to,f}$ density (pA/pF) n=	28.6 ± 3.3 *13*	15.6 ± 2.6 * *22*	16.0 ± 5.0 * *13*
$I_{to,f}$ inac (ms) n=	116.0 ± 8.0 *13*	94.0 ± 10.0 *22*	108.0 ± 10.0 *13*
$I_{K,slow}$ density (pA/pF) n=	25.0 ± 3.6 *13*	9.1 ± 0.8 * *22*	8.7 ± 0.9 * *13*
$I_{K,slow}$ inac (ms) n=	1214 ± 105 *13*	1300 ± 82 *22*	1268 ± 120 *13*
I_{SS} density (pA/pF) n=	5.6 ± 0.6 *13*	4.7 ± 0.3 *22*	4.0 ± 0.4 *13*
I_{K1} density (pA/pF) n=	-3.0 ± 0.2 *17*	-3.0 ± 0.3 *22*	-3.6 ± 0.5 *13*
$I_{Ca,L}$ density (pA/pF) n=	-10.9 ± 0.7 *20*	-7.5 ± 0.6 * *15*	-7.6 ± 0.6 * *16*
Fast $I_{Ca,L}$ inac (ms) n=	4.6 ± 0.2 *20*	6.4 ± 0.5 * *15*	5.2 ± 0.3 * *16*
Slow $I_{Ca,L}$ inac (ms) n=	86.5.0 ± 5.2 *20*	99.8 ± 8.9 * *15*	101.6 ± 4.5 * *16*
$I_{Ca,L}$ st st inac (mV) n=	-30.0 ± 0.4 *20*	-26.4 ± 0.6 * *15*	-24.4 ± 0.5 * *14*

Supplementary Table S4: Survival during experimental protocol.

	Treatment Period	Arrhythmogenic test 1 (under treatment)	Arrhythmogenic test 2 (treatment stopped)	End of Protocol (5 weeks after arrhythmogenic test 2)
Sham	12	12	12	11(¤)
PMI	12	12	12	7*
BNP-PMI	12	12	8	5†
BB-PMI	12	12	12	8*
BB-BNP-PMI	12	12	12	11‡§